Cellular and Molecular Life Sciences (2023) 80:308
https://doi.org/10.1007/s00018-023-04961-y

Cellular and Molecular Life Sciences

ORIGINAL ARTICLE

Omentin-1 induces mechanically activated fibroblasts lipogenic differentiation through pkm2/yap/pparγ pathway to promote lung fibrosis resolution

Yunna Zhang[1] · Jiafeng Fu[1] · Chen Li[2] · Yanfen Chang[1] · Xiaohong Li[3] · Haipeng Cheng[3] · Yujia Qiu[1] · Min Shao[1] · Yang Han[1] · Dandan Feng[1] · Shaojie Yue[4] · Zhengwang Sun[6] · Ziqiang Luo[1,5] · Yan Zhou[1]

Received: 22 June 2023 / Revised: 9 September 2023 / Accepted: 11 September 2023 / Published online: 28 September 2023

Abstract

Idiopathic pulmonary fibrosis (IPF) is a progressive and fatal lung disease characterized by extensive extracellular matrix (ECM) deposition by activated myofibroblasts, which are specialized hyper-contractile cells that promote ECM remodeling and matrix stiffening. New insights on therapeutic strategies aimed at reversing fibrosis by targeting myofibroblast fate are showing promise in promoting fibrosis resolution. Previously, we showed that a novel adipocytokine, omentin-1, attenuated bleomycin (BLM)-induced lung fibrosis by reducing the number of myofibroblasts. Apoptosis, deactivation, and reprogramming of myofibroblasts are important processes in the resolution of fibrosis. Here we report that omentin-1 reverses established lung fibrosis by promoting mechanically activated myofibroblasts dedifferentiation into lipofibroblasts. Omentin-1 promotes myofibroblasts lipogenic differentiation by inhibiting dimerization and nuclear translocation of glycolytic enzymes pyruvate kinase isoform M2 (PKM2) and activation of the downstream Yes-associated protein (YAP) by increasing the cofactor fructose-1,6-bisphosphate (F1, 6BP, FBP). Moreover, omentin-1 activates proliferator-activated receptor gamma (PPARγ) signaling, the master regulator of lipogenesis, and promotes the upregulation of the lipogenic differentiation-related protein perilipin 2 (PLIN2) by suppressing the PKM2-YAP pathway. Ultimately, omentin-1 facilitates myofibroblasts transformation into the lipofibroblast phenotype, with reduced collagen synthesis and enhanced degradation properties, which are crucial mechanisms to clear the ECM deposition in fibrotic tissue, leading to fibrosis resolution. Our results indicate that omentin-1 targets mechanical signal accelerates fibrosis resolution and reverses established lung fibrosis by promoting myofibroblasts lipogenic differentiation, which is closely associated with ECM clearance in fibrotic tissue. These findings suggest that targeting mechanical force to promote myofibroblast lipogenic differentiation is a promising therapeutic strategy against persistent lung fibrosis.

Keywords Omentin-1 · Pulmonary fibrosis · Myofibroblast · Extracellular matrix stiffness · Lipofibroblast

✉ Ziqiang Luo
luoziqiang@csu.edu.cn

✉ Yan Zhou
zhouyanxy@csu.edu.cn

1 Department of Physiology, Xiangya School of Medicine, Central South University, Changsha 410008, Hunan, China

2 Department of Physiology, Changzhi Medical College, Changzhi 046000, China

3 Department of Pathology, The Second Xiangya Hospital, Central South University, Changsha 410013, China

4 Department of Pediatrics, Xiangya Hospital, Central South University, Changsha 410013, China

5 Hunan Key Laboratory of Organ Fibrosis, Changsha 410013, China

6 Center for Immunology and Inflammatory Diseases, Division of Pulmonary and Critical Care Medicine, Massachusetts General Hospital, Harvard Medical School, Boston, MA, USA

Introduction

Idiopathic pulmonary fibrosis (IPF) is a chronic, progressive and non-reversible interstitial lung disease, characterized by progressive dyspnea, bilateral interstitial infiltrates, and restrictive physiology on pulmonary function testing [1]. Epidemiological studies reveal that the incidence of IPF is estimated between 5 and 20 cases per 100,000, with a mean survival of 3–5 years following diagnosis [2]. There are only two medications, pirfenidone and nintedanib, for IPF, approved by the Food and Drug Administration, which can modestly lower the rate of lung function deterioration but do not halt or reverse disease progression or reduce mortality [3, 4]. For the translational medical research on pulmonary fibrosis in vivo, there is an urgent requirement for treatments that can not only alleviate reversible models of pulmonary fibrosis but also accelerate its regression and reverse the degree of pulmonary fibrosis in non-reversible models, which are more representative of the pathogenesis of IPF.

Extensive extracellular matrix (ECM) plays an essential role in perpetuating fibrotic pathologies [5]. Therefore, the locoregional clearance of the intrapulmonary ECM is of utmost importance to reverse the progression of this devasting disease [6]. Myofibroblasts play an important role in the synthesis of ECM and in force generation, which, during the normal tissue repair process, results in wound healing and ECM reorganization, and is also a critical component in the formation of fibrosis [7]. The fate of activated myofibroblasts in injured tissue may ultimately determine whether normal healing occurs or progression to end-stage fibrosis occurs. Targeting myofibroblast apoptosis, deactivation or cellular immunoclearance are new therapeutic strategies aimed at reversing fibrosis [8]. Recent research showed that metformin alters the fate of myofibroblasts and accelerates fibrosis resolution by inducing myofibroblast deactivation and transition to a lipofibroblast phenotype, which is a relatively quiescent fibroblasts form with upregulation of proliferator-activated receptor gamma (PPARγ) and intracellular lipid droplets [9]. Single-cell transcriptomics and recent studies have shown that lipofibroblasts are a poorly differentiated phenotype that synthesize less collagen than myofibroblasts [10–12], however, the effect or mechanism of lipofibroblasts on the regulation of collagen synthesis and degradation in pulmonary fibrosis remain unknown.

Omentin-1, also known as "intelectin-1," an adipokine encoded by the ITLN1 gene, is a recently identified adipokine that regulates inflammation, vasomotor and endothelial function, cell proliferation, apoptosis, and cell differentiation [13]. A single-dose bleomycin (BLM)-induced pulmonary fibrosis animal model is widely used in lung fibrosis research, which leads to ECM deposition, and the development of fibrosis in lung tissue with a fibrosis peak around 14–21 days following BLM administration, which then spontaneously resolves [12, 14, 15]. Our previous study indicated that omentin-1 was significantly upregulated at 21 days following BLM stimulation. However, omentin-1 deletion exacerbated BLM-induced pulmonary fibrosis, and overexpression of omentin-1 attenuated lung injury [16] and pulmonary fibrosis [17]. These findings indicated that omentin-1 could potentially be used as an antifibrosis treatment, while the role and mechanism of the increased omentin-1 level during the fibrosis peak stage of the reversible fibrosis model are unknown. Moreover, the effect of omentin-1 on non-reversible pulmonary fibrosis and IPF is unknown.

Based on these findings, we further hypothesized that the increased level of omentin-1 during the fibrosis peak stage could be an important endogenous factor in promoting the resolution of reversible pulmonary fibrosis induced by single-dose BLM, and exogenous supplementation of omentin-1 may reverse established lung fibrosis in a non-reversible model. Here, we demonstrate that omentin-1 was significantly increased during the regressive fibrotic stage 42 days following single-dose BLM stimulation, by which time the degree of fibrosis largely resolved. Overexpression of omentin-1 significantly accelerates the regression of reversible pulmonary fibrosis at 42 days and promotes the resolution of non-reversible pulmonary fibrosis. We furthermore show that omentin-1 significantly stimulates myofibroblasts induced by transforming growth factor β (TGF-β), or high matrix stiffness transdifferentiating to lipofibroblasts in vitro, as well as increases the number of lipofibroblasts in the lung tissues in both the reversible and non-reversible fibrosis models, accompanied by a decreased number of α-smooth muscle actin $(\alpha\text{-SMA})^+$ myofibroblasts. Conclusively, omentin-1 upregulates the level of the metabolite fructose-1,6-bisphosphate (F1, 6BP, FBP), further reduces the glycolytic enzyme pyruvate kinase isoform M2 (PKM2) dimer to inhibit the binding with Yes-associated protein (YAP) and its nuclear translocation. We further show that omentin-1 significantly upregulates the lipogenic differentiation regulator PPARγ, promoting myofibroblasts deactivation to lipofibroblasts via inhibition of PKM-YAP signaling. Significantly, we illustrate that an increased number of lipofibroblasts, which have decreased collagen synthesis property and increased collagen degradation capacity, can turnover collagen deposition in fibrotic tissue. Overall, these findings indicate the therapeutic potential of exogenous omentin-1 in treating established lung fibrosis induced by BLM, which could potentially be translated to treating IPF patients.

Materials and methods

Research design

The goals of this study were threefold: to identify the effect of omentin-1 on reversible and non-reversible lung fibrosis; to determine whether targeting myofibroblast fate ameliorates fibrosis; how omentin-1 promotes lipogenic differentiation of myofibroblast and how lipofibroblast contributing fibrosis resolution. For in vivo mouse studies, single-dose BLM-induced reversible lung fibrosis, non-reversible fibrosis including repetitive BLM injured model and single-dose BLM in aged mice model were chosen as well-established and relevant models of lung fibrosis. Sample sizes were calculated by power analysis based on previous experience and feasibility. A minimum of four mice were included in each group. Mice were randomly assigned to treatment groups. Biochemical and histological outcomes were analyzed with the investigator blinded to the treatment groups and no animals were excluded as outliers from the reported dataset. In cell-based assays, we treated fibroblasts stimulated by TGF-β or matrix stiffness with omentin-1 and observed a pronounced shift in their phenotype from myofibroblast to lipofibroblast which contained lipid droplets. All in vitro and in vivo experiments were performed in three to four technical replicates. The number of biologically independent samples and/or biologically independent experiments is identified in each figure legend.

Animal experiments

All animals were housed under specific pathogen-free (SPF) conditions with free access to food and water. Briefly, for the reversible model, male C57BL/6j mice (8 weeks, 21–24 g) received an intratracheal instillation of BLM (1.25 mg/kg, Nippon Kayaku, Tokyo, Japan). Omentin-1 treated group mice were intravenously injected with 100 μL of Adenovirus-*ITLN1* (Ad-*ITLN1*) suspension (virus titer > 10^9 PFU/mL) blend with 100 μL normal saline at 11 days and 25 days after BLM challenge. Control mice and peak fibrosis (14 d.p.i) or reversible-fibrosis (42 d.p.i.) mice were injected with an equal volume of Ad-β-gal suspension. For the repeated injury model, 8 weeks male mice were subjected to oropharyngeal aspiration (OPA) of saline or BLM (1.0 mg/kg) once per week for 8 weeks. Ad-*ITLN1* or Ad-β-gal was administrated at 25 d.p.i and 39 d.p.i. For non-regression pulmonary fibrosis model in aging mice, 18–24 months mice were intratracheally injected with BLM (1.25 mg/kg) to induce pulmonary fibrosis, Ad-*ITLN1* or Ad-β-gal was injected at 11 d.p.i. Lungs were harvested on day 21. All animal experiments were approved by the local authorities (The ethics committee of the Central South University Science Research Center; Changsha, China) and performed in accordance with the guidelines of the National Institutes of Health for the Care and Use of Laboratory Animals.

Polyacrylamide hydrogels (PAAm)

Polyacrylamide hydrogels were prepared as described previously [18]. Briefly, prepare chlorosilylated glass slides, mix 40% w/v acrylamide and 2% w/v bisacrylamide to obtain a final concentration ratio of 3:0.11 (0.4 kPa), 7.5:0.05 (1.6), 12:0.24 (25 kPa) or 12:1 (100 kPa) to prepare PAAm gels, mixed with TEMED and ammonium persulfate to polymerize the gels. Quickly transfer 50 μL of solution to the hydrophobic slide and cover it with treated cover glass. After polymerized, the gels were rinsed three times with 50 mM HEPES (pH 8.5). Active hydrogels with 0.25 mg/ml sulfo-SANPAH (ProteoChem, USA) under 365 nm UV light, next coated with 40 ug/ml collagen overnight at 4 °C. The gels were sterilized with ultraviolet light and washed with PBS before cell inoculation. Atomic force microscopy was used to determine the stiffness of the hydrogels by indentation.

Cell culture

Mouse Fibroblast cell line NIH/3T3 was purchased from Procell Life Science & Technology (Wuhan, China). Cells were maintained at 37 °C, 5% CO_2 in Dulbecco modified eagle medium (DMEM; Procell) supplemented with 10% fetal bovine serum (FBS; Sigma), 0.2% NaHCO3, 100 μg/ml streptomycin, and 100 IU/ml penicillin. For TGF-β1 activation, cells were pretreated for 1 h with recombinant omentin-1 (500 ng/ml, R&D Systems, USA) and were activated by culturing in TGF-β1 (10 ng/ml) for 48 h. For stiff matrix pre-activation, cells were cultured on the soft or stiff matrix for 48–72 h and then omentin-1 (500 ng/ml) administration for another 48–72 h. In some experiments, GW9662 (10 μM, Selleck, China) was added for 2 h to show the effect of inhibition of the PPARγ pathway. FBP (0.6 mM, Apexbio, China) was used for supplementation.

Plasmid transfections

YAP1 (GenBank accession no. NM-001171147) cDNA was synthesized by GENECHEM (Shanghai, China) and constructed into pIRES2 vector. Cells were grown to 70% confluence and transfected with 1 μg of the YAP1 plasmid or control vector using Lipofectamine 3000 (Invitrogen) according to the manufacturer's instructions.

Histological assessment of pulmonary fibrosis

Lung tissues were fixed in 4% paraformaldehyde in Phosphate Buffer Saline (PBS), embedded in paraffin. Hematoxylin and eosin (H&E) and Masson's trichrome staining were performed using standard procedures.

RNA extraction and q-PCR experiments

Total RNA from cell samples was isolated using TRIzol reagent (Takara, Japan) and reversed transcribed using a 5× TransScript® Uni All-in-One SuperMix for qPCR (Transgene, China) according to the manufacturers' instructions. Real-time PCR was performed using PerfectStart® Green qPCR SuperMix (Transgene, China) and detected with a Bio-Rad real-time PCR system (CFX96 Touch™, Bio-Rad, USA). Relative gene expression was expressed as the relative fold of expression level in the control group. The primer sequences for omentin-1, α-SMA, collagen I (Col 1), and collagen III (Col 3), fibronectin (FN), PLIN2, LOXL1, LOXL3, LOXL4, CTSK, PLAT, PLAU, MMP14, HK2, PKM2, LDHA, PPARγ were listed in Table S1.

Immunoblot, non-denaturing PAGE and co-immunoprecipitation

Total protein lysates were prepared in cold RIPA lysis buffer (Bioss, China) containing a proteinase inhibitor cocktail (Apexbio, USA) for 30 min. Lysates were clarified by centrifugation at 12,000×*g* for 10 min. 20 µg protein per sample was separated by sodium dodecyl sulfate–polyacrylamide gel electrophoresis (SDS-PAGE), transferred to polyvinylidene fluoride (PVDF) membranes, and then probed with the indicated antibodies overnight at 4 °C. β-Actin or β-tubulin was used as a loading control. HRP-conjugated anti-rabbit IgG (1:5000; Signalway Antibody, USA) and HRP-conjugated anti-mouse IgG (H + L) (1:5000; Signalway Antibody, USA) were used as secondary antibodies for 1 h at room temperature (RT). Subsequently, membranes were covered with enhanced chemiluminescence reagents (Cwbio, China) and imaged immediately using ChemiDoc XRS + (Bio-Rad Laboratories). The primary antibodies were as follows: anti-β-actin (1:3000; Proteintech, China), anti-β-tubulin (1:5000; Proteintech, China), anti-α-SMA (1:1000; Servicebio, China), anti-collagen III (Col 3) (1:1000; Proteintech, China), anti-collagen I (Col 1) (1:1000; Proteintech, China), anti-Fibronectin (FN) (1:1000; Proteintech, China), anti-HK2 (1:1000; Cell Signaling Technology, USA), PKM2 (1:3000; Cell Signaling Technology, USA) and LDHA (1:1000; Cell Signaling Technology, USA).

For CO-IP, crude lysates of 1×10^7 cells were incubated with Protein A/G Plus-SefinoseTM Resin (Sangon Biotech, China) according to the manufacturer's instructions. Briefly, cell/tissue lysates were incubated with capture buffer containing 1 ug YAP antibody (Santa cruz, USA) and shaken by vibration at RT for 2 h. Beads were washed with wash buffers 1 and 2 and resuspended in 2 × SDS buffer and protein–protein complexes were later subjected to Western blot.

For non-denaturing analysis, cells were lysed in an NP40 buffer (150 mM NaCl, 50 mM Tris–HCl pH 7.4, 1% NP40). Nondenaturing PAGE was performed on 8% (w/v) acrylamide nondenaturing gels using 4 × loading buffer without SDS and β-mercaptoethanol. Membranes were probed with anti-PKM2 (1:3000, Cell Signaling Technology, USA) and revealed with HRP-conjugated anti-mouse antibodies.

Immunohistochemistry and immunofluorescence

Mouse lungs were fixed with 4% paraformaldehyde/PBS solution and embedded in paraffin. 5-µm-thick sections deparaffinized in serial solutions of xylene, gradient ethanol and water, followed by antigen retrieval by steaming in 1 mM EDTA for 5 min in a pressure cooker followed by a 1 h cooling period to room temperature. The lung sections were washed with PBS buffer and blocked with 5% BSA for 30 min. Next, blocked samples were incubated with mouse anti-α-SMA (1:200; Servicebio, China), anti-collagen I (1:200, Proteintech, China), anti-PLIN2 antibody (1:200, Abcam, USA) and vimentin antibody (1:200, HUABIO, China) overnight at 4 °C followed by exposure to species-appropriate secondary antibodies anti-rabbit IgG (Alexa Fluor 488 conjugate) (1:200, Proteintech, China) or Alexa Fluor® 594 AffiniPure Goat Anti-Mouse IgG (H + L) (1:200, Jackson ImmunoResearch, USA) in PBS for 1 h at room temperature. Slides were then counterstained with nuclear dye DAPI and mounted. For cell immunofluorescence, cells were grown on coverslips or hydrogels coated coverslips and The fixed with 4% paraformaldehyde for 15 min and permeabilized with 0.01% Triton. The cells were blocked with 5% BSA for 30 min, and stained overnight at 4 ◦C with indicated antibodies and secondary antibodies. Images were acquired on a fluorescence microscopic imaging system (Leica, Germany).

For Immunohistochemistry, after paraffin tissue sections were deparaffinized and repaired by a pressure cooker, then incubated with 3% hydrogen peroxide for 10 min to inhibit endogenous peroxidase activity. The sections were stained with primary antibodies against PKM2 (1:400, Cell Signaling Technology, USA), phospho-PKM2 (Tyr105) (1:400, Affinity, China), PLIN2 (1:200, Abcam, USA) or PPARγ (1:200, Zen-bioscience, China) overnight at 4 °C, followed by incubation with an HRP-conjugated secondary antibody (1:100; Sigma-Aldrich, USA) at room temperature for 30 min. DAB staining is implemented, hematoxylin is used to indicate nucleus.

Collagen hybridizing peptide (CHP) staining

To visualize the degraded collagen, CY3-CHP (3Helix, USA) analysis is implemented according to the manufacturer's instructions. Removing the embedding of paraffin with standard procedures. Block sections with 5% BSA. Heat the dilute CHP solution (15 μM) in a sealed microtube at 80 °C for 5 min. Quench the solution to room temperature and incubate the tissues with the staining solution at 4 °C overnight. Images were captured with a Leica microscope.

Nile red staining for lipid droplets

Cells were fixed in a 4% buffered paraformaldehyde solution. For lipid droplet staining, cells were incubated with 1 μM Nile Red for 5–10 min at RT. After washing with PBS, DAPI was used to stain nuclei followed by washes with PBS. Images were captured with a Leica microscope.

Metabolomics

Cells were freeze-dried and resuspended with prechilled 80% methanol by well vortex. Then the samples were incubated on ice for 5 min and centrifuged at 15,000*g*, 4 °C for 15 min. Some of the supernatant was diluted to a final concentration containing 53% methanol by LC–MS grade water. The samples were subsequently transferred to a fresh Eppendorf tube and then were centrifuged at 15,000*g*, 4 °C for 15 min. Finally, the supernatant was injected into the LC–MS/MS system analysis UHPLC-MS/MS analyses were performed using a Vanquish UHPLC system (ThermoFisher, Germany) coupled with an Orbitrap Q ExactiveTMHF-X mass spectrometer (Thermo Fisher, Germany) in Novogene Co., Ltd. (Beijing, China).

Single-cell transcriptomic analyses

Raw CEL files for GSE135893 were downloaded from GEO. Data was processed using the Seurat R package. Cell types were assigned based on the published metadata [19]. Fibroblast counts data were log-normalized, variable genes quantified and principal component analysis performed on these variable genes. The Find markers function in the R 3.6.3 software was used to screen for differentially expressed genes.

Statistical analysis

All data are presented as means ± the standard deviations (SD). Statistical comparisons between the two groups were analyzed with an unpaired Student's t-test. Comparisons among multiple groups were analyzed with one-way ANOVA, followed by the Student–Newman–Keuls test using GraphPad Prism software (GraphPad Software, San Diego, CA). Correlation between variables was determined using a Pearson correlation analysis. The difference between groups was significant if $p < 0.05$.

Results

Omentin-1 accelerates regression of single-dose BLM-induced self-resolving pulmonary fibrosis

Single-dose BLM-induced pulmonary fibrosis is characterized by spontaneous resolution of the fibrosis, starting approximately 14–21 days post instillation (d.p.i.) [12, 14, 15]. Hematoxylin and eosin (H&E) and Masson staining demonstrated that destruction of the lung structure and accumulation of collagen in the lung tissue were significantly attenuated at 42 d.p.i. when compared to that at 14 d.p.i. and 21 d.p.i. (Fig. 1a). Furthermore, the Ashcroft score, which is used to grade lung fibrosis, showed a significantly decreased at 42 d.p.i. (Fig. 1b). In our previous study, the mRNA level of omentin-1 increased in BLM-induced lung fibrosis at both 14 d.p.i. and 21 d.p.i. [17]. Here, the mRNA level of omentin-1 was further upregulated at 42 d.p.i. (Fig. 1c). Collectively, our research showed that the gene expression of omentin-1 was negatively correlated with the Ashcroft score (Fig. 1d), indicating that the increased expression of omentin-1 may be an endogenous antifibrosis factor responsible for promoting the resolution of pulmonary fibrosis.

Our previous study indicated that omentin-1 deletion exacerbated BLM-induced pulmonary fibrosis, and overexpression of omentin-1 attenuated pulmonary fibrosis at the fibrotic peak stage prior to self-regression [17]. To further investigate its potential role in the regression process, we examined the effect of omentin-1 overexpression on fibrosis regression at 42 d.p.i. in the single-dose BLM-induced self-resolving pulmonary fibrosis model (Fig. 1e, f). Prior to this, it has been demonstrated that overexpression of omentin-1 does not affect the structure of lung tissue nor the deposition of collagen within the interstitial (Fig. S1A, B). Fibrosis resolution at 42 d.p.i. was confirmed using H&E and Masson staining, and was further accelerated by overexpression of omentin-1 (Fig. 1g). Moreover, a significant downregulation of ECM components, including collagen I (Col 1), collagen III (Col 3) and fibronectin (FN) were observed at 42 d.p.i. compared to that at 14 d.p.i., and omentin-1 overexpression further reduces these ECM components at both the mRNA and protein levels (Fig. 1h, i). These results indicated that omentin-1 accelerates the regression of self-resolving pulmonary fibrosis.

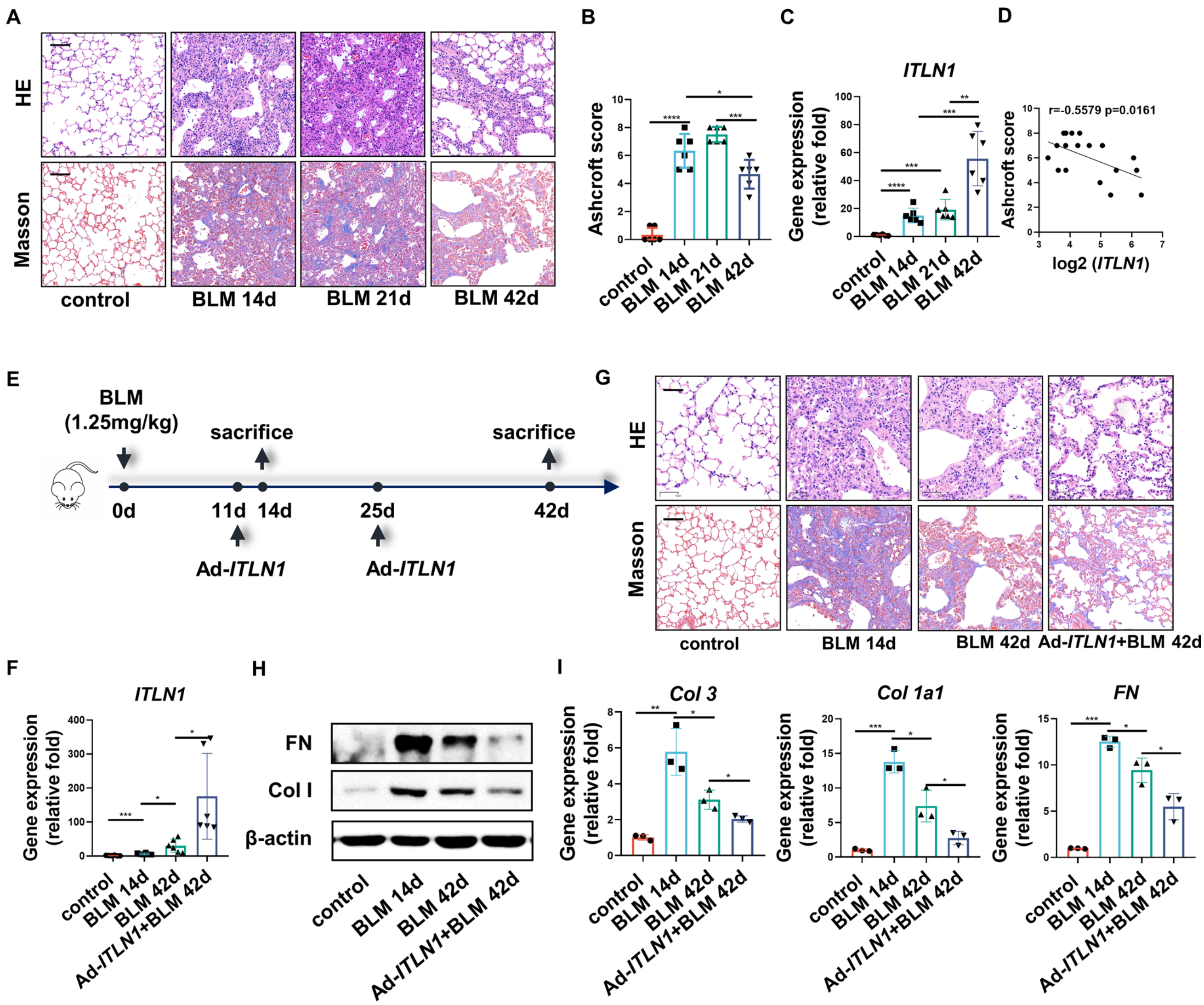

Fig. 1 Omentin-1 accelerates regression of pulmonary fibrosis in reversible model. (**a**) Representative micrographs of H&E and Masson staining of lung sections, scale bar = 50 μm ($n=6$). (**b**) Ashcroft score to grade fibrosis scale ($n=6$). (**c**) The mRNA level of omentin-1 in the different phases of fibrotic lung tissue of mice detected by qPCR ($n=6$). (**d**) The correlation between Ashcroft score and omentin-1 mRNA level following BLM injury. (**e**) Schematic for single-dose BLM-induced reversible fibrosis model and overexpression of omentin-1. (**f**) The mRNA level of omentin-1 in the lung tissue of mice detected by qPCR ($n=6$). (**g**) Representative micrographs of H&E and Masson staining of lung sections, scale bar = 50 μm ($n=6$). (**h**) The content of FN and Col 1 in lung tissue detected by western blotting. β-actin was used as the loading control ($n=3$). (**i**) The mRNA level of Col 3, Col 1, and FN in lung tissue detected by qPCR ($n=3$)

Omentin-1 reverses BLM-induced non-reversible pulmonary fibrosis

IPF is an age-associated progressive fibrotic interstitial lung disease. Thus, non-reversible models are more comparable to the pathogenesis of IPF and more representative for testing the treatment strategies. Researches shows that repetitive intranasal BLM instillation in young mice [20] and single-dose BLM instillation in aged mice [15] is characterized by persistent progressive pulmonary fibrosis, with a deficiency in the capacity for lung fibrosis resolution. These two models were established to investigate whether overexpression of omentin-1 promotes fibrosis resolution (Fig. 2a, f). Overexpression of omentin-1 was confirmed by upregulation of omentin-1 mRNA in the lung tissue of these two models (Fig. 2b, g). Repetitive intranasal BLM administration in young mice and single-dose BLM administration in aged mice induced alveolar wall thickening, dense fibrosis and interstitial collagen deposition, shown using H&E and Masson staining, which appears to be mitigated by overexpression of omentin-1 (Fig. 2c, h). Furthermore, the increased mRNA and protein level of ECM components (Col 1, Col

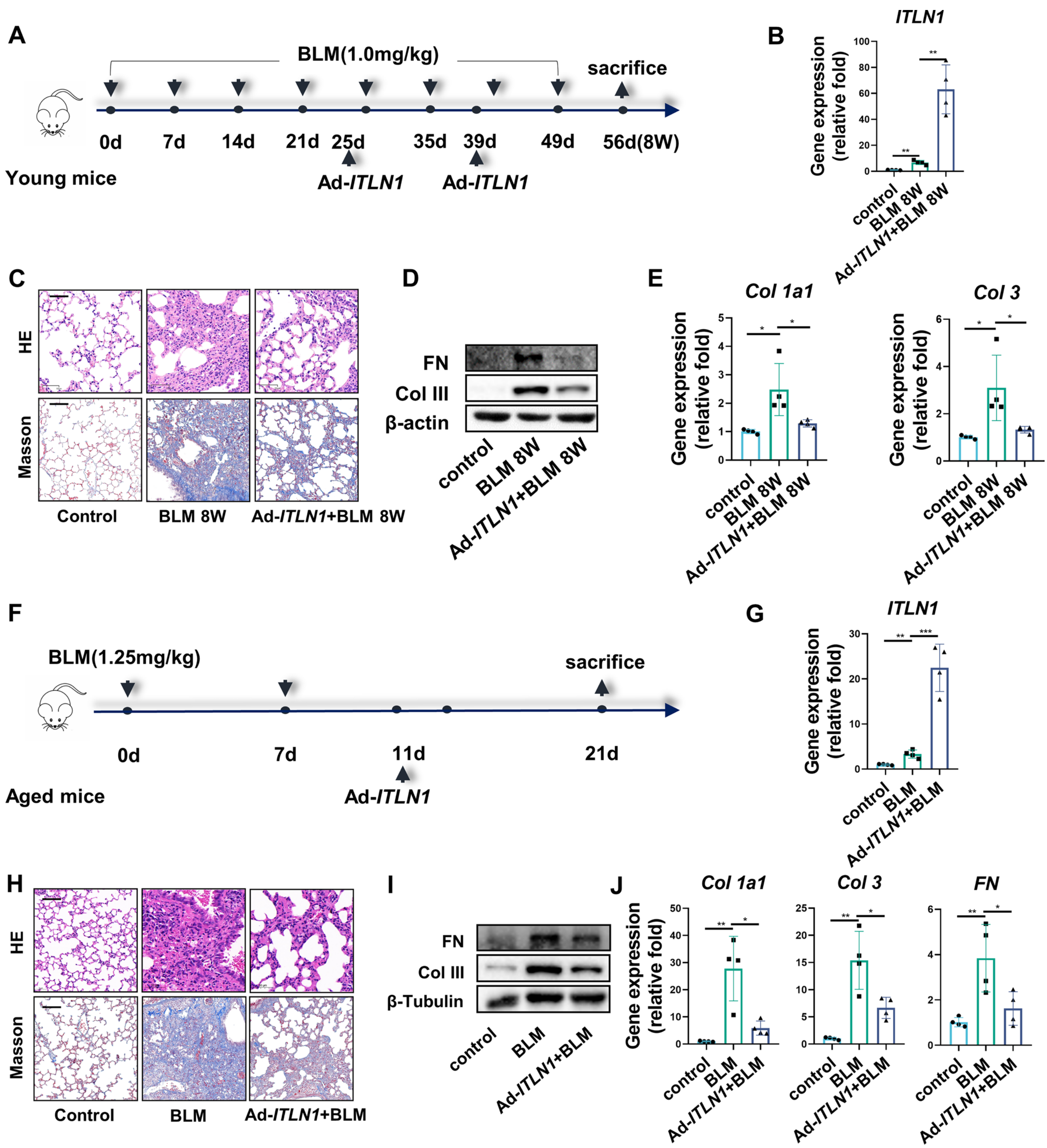

Fig. 2 Omentin-1 reverses non-reversible pulmonary fibrosis. (**a, f**) Schematic for non-reversible fibrosis preparation procedure including repetitive BLM injured model and single-dose BLM in aged mice model. (**b, g**) The mRNA level of omentin-1 in the lung tissue of mice detected by qPCR ($n=4$). (**c, h**) Representative micrographs of H&E and Masson staining of lung sections from indicated groups of mice, scale bar = 50 μm ($n=4$). (**d, i**) The content of FN and Col 3 in lung tissue detected by western blotting. β-actin or β-tubulin were used as the loading control ($n=3$). (**e, j**) The mRNA level of Col 1, Col 3, FN in lung tissue detected by qPCR ($n=4$)

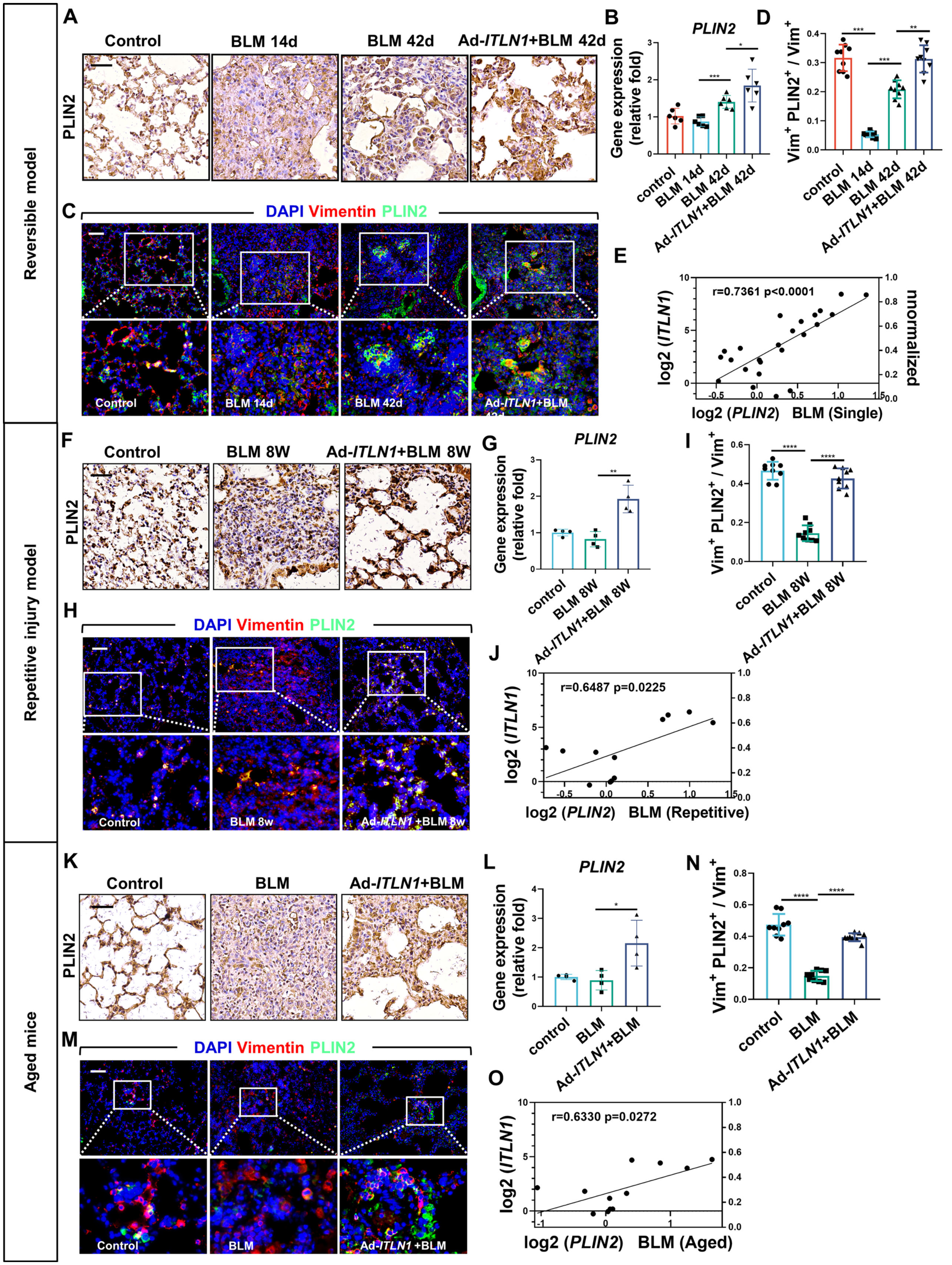
Reversible model
A
Control
BLM 14d
BLM 42d
Ad-ITLN1+BLM 42d
PLIN2
B
PLIN2
Gene expression (relative fold)
control
BLM 14d
BLM 42d
Ad-ITLN1+BLM 42d
D
Vim+ PLIN2+ / Vim+
C
DAPI Vimentin PLIN2
Control
BLM 14d
BLM 42d
Ad-ITLN1+BLM 42d
E
r=0.7361 p<0.0001
log2 (ITLN1)
nnormalized
log2 (PLIN2) BLM (Single)
Repetitive injury model
F
Control
BLM 8W
Ad-ITLN1+BLM 8W
PLIN2
G
PLIN2
Gene expression (relative fold)
control
BLM 8W
Ad-ITLN1+BLM 8W
I
Vim+ PLIN2+ / Vim+
H
DAPI Vimentin PLIN2
Control
BLM 8w
Ad-ITLN1 +BLM 8w
J
r=0.6487 p=0.0225
log2 (ITLN1)
log2 (PLIN2) BLM (Repetitive)
Aged mice
K
Control
BLM
Ad-ITLN1+BLM
PLIN2
L
PLIN2
Gene expression (relative fold)
control
BLM
Ad-ITLN1+BLM
N
Vim+ PLIN2+ / Vim+
M
DAPI Vimentin PLIN2
Control
BLM
Ad-ITLN1 +BLM
O
r=0.6330 p=0.0272
log2 (ITLN1)
log2 (PLIN2) BLM (Aged)

◂**Fig. 3** Omentin-1 increases lipofibroblasts in reversible and non-reversible fibrotic lung tissue. (**a, f, k**) Immunohistochemistry staining of PLIN2 in the lung tissue of mice, scale bar = 50 μm (n = 3). (**b, g, l**) The mRNA level of PLIN2 in the lung tissue detected by qPCR (n ≥ 4). (**c, h, m**) Immunofluorescent double-staining of vimentin (Red) and PLIN2 (Green) of lung sections of mice, scale bar = 50 μm (n = 3). (**d, I, n**) Quantification of the percentage of lipofibroblasts in fibroblast (Vimentin$^+$PLIN2$^+$ cells/Vimentin$^+$ cells) according to immunofluorescent image. (**e, j, o**) The correlation between PLIN2 and omentin-1 mRNA level following BLM injury

3 and FN) following BLM insult in these two models were also diminished by omentin-1 overexpression (Fig. 2d, e, i, j). Together, all these results demonstrate that omentin-1 effectively promotes the regression of non-reversible fibrosis.

Omentin-1 accommodates regression of pulmonary fibrosis by increasing lipofibroblasts in fibrotic lung tissue

Myofibroblasts are the most important effector cells in pulmonary fibrosis pathogenesis, which is characterized by a high level of α-SMA. Our previous work showed that the number of α-SMA$^+$ myofibroblasts decreased following omentin-1 administration in the self-resolving pulmonary fibrosis model [17]. Concordantly, the number of myofibroblasts was also downregulated by omentin-1 overexpression in both the reversible and non-reversible lung fibrosis models in this study. Furthermore, the gene expression of omentin-1 was inversely proportional to the mRNA level of α-SMA in three fibrosis models (Fig. S1C–N).

Apoptosis, deactivation, and reprogramming of myofibroblasts are important processes in the resolution of fibrosis [8]. As the above results show, there is a significant decrease in the number of myofibroblasts in lung fibrosis tissue following overexpression of omentin-1 in vivo. Research shows that activated myofibroblasts can dedifferentiate into lipofibroblasts (lipogenic differentiation) during fibrosis resolution which is a relatively quiescent fibroblast [12]. Subsequent studies have confirmed that metformin promotes lipogenic differentiation of lung myofibroblasts to reverse lung fibrosis [9]. To verify whether lipogenic differentiation is involved in the accelerated resolution process of the reversible fibrosis model caused by omentin-1, we analyzed the level of the lipogenic differentiation marker perilipin 2 (PLIN2) and the number of PLIN2$^+$ lipofibroblasts in the lung tissue. Immunohistochemistry and quantitative polymerase chain reaction (qPCR) results showed that BLM decreased the level of PLIN2 at 14 d.p.i., PLIN2 then increased in the fibrosis resolving phases at 42 d.p.i. and was effectively further upregulated by omentin-1 (Fig. 3a, b). In addition, BLM stimulation diminished the number of lipofibroblasts at the peak of fibrosis at 14 d.p.i., indicated by PLIN2 (green) and vimentin (red) double staining. Subsequently, an augmented number of PLIN2$^+$vimentin$^+$ lipofibroblasts emerged at 42 d.p.i., which was further increased by overexpression of omentin-1 (Fig. 3c, d). Moreover, we obtained theoretically consistent results in the two of non-reversible fibrosis models. Decreased levels of PLIN2 and numbers of lipofibroblasts were observed following BLM administration, which were effectively recovered by omentin-1 (Fig. 3f–i, k–n). Notably, there was a significant positive correlation between the gene expression of omentin-1 and PLIN2 (Fig. 3e, j, o). Collectively, these results indicate that omentin-1 may lead to fibrosis regression by increasing the number of lipofibroblasts in fibrotic lung tissue.

Omentin-1 induces lipogenic differentiation of lung myofibroblasts in vitro

We previously demonstrated that omentin-1 pretreatment reduces the expression of α-SMA, Col 1, and FN in TGF-β1-activated myofibroblasts [17], which is consistent with the results of this study (Fig. S1O, P). In addition, omentin-1 promotes the expression of the lipogenic differentiation marker PLIN2 in myofibroblasts activated by TGF-β1, indicating omentin-1 may induce lipogenic differentiation of myofibroblasts (Fig. S1Q). Matrix stiffness plays a critical role in the development of fibrosis. For instance, Young's modulus of the normal lung tissues is 0.4–5 kPa, which is elevated to 25 kPa in fibrotic lungs [18, 21]. To explore the effect of omentin-1 on activated myofibroblast stimulated by increased stiffness, we established in vitro pre-activation myofibroblast model using polyacrylamide hydrogels [18]. Consequently, high stiffness-induced myofibroblasts activation was indicated by the upregulated protein levels of collagen and α-SMA (Fig. 4a, b). Omentin-1 was administered to fibroblasts cultured on both soft and stiff substrates (Fig. 4c). The results indicated that omentin-1 elicits minimal effects on quiescent fibroblasts on a soft matrix, but effectively reversed the increased level of α-SMA and FN and blunted the induction of Col 3 mRNA in high matrix stiffness-treated fibroblasts (Fig. 4d, e). Actin filament (F-actin) assembly can contribute to high contraction and cell tension in myofibroblasts. Phalloidin stainning for F-actin demonstrated that high matrix stiffness-induced high F-actin assembly could be reversed with omentin-1 (Fig. 4f). Our results showed that omentin-1 increases the number of lipofibroblasts in vivo, suggesting it likely controls the fate of myofibroblasts that have been deactivated into lipofibroblasts. Fluorescence staining showed that omentin-1 administration decreased the number of α-SMA$^+$ myofibroblasts and increased the number of PLIN2$^+$ lipofibroblasts as well as the mRNA level of PLIN2 in stiffness-stimulated fibroblasts (Fig. 4g–i). Moreover, omentin-1 significantly increases the quantity of lipid droplets in stiffness-stimulated fibroblasts, which is a

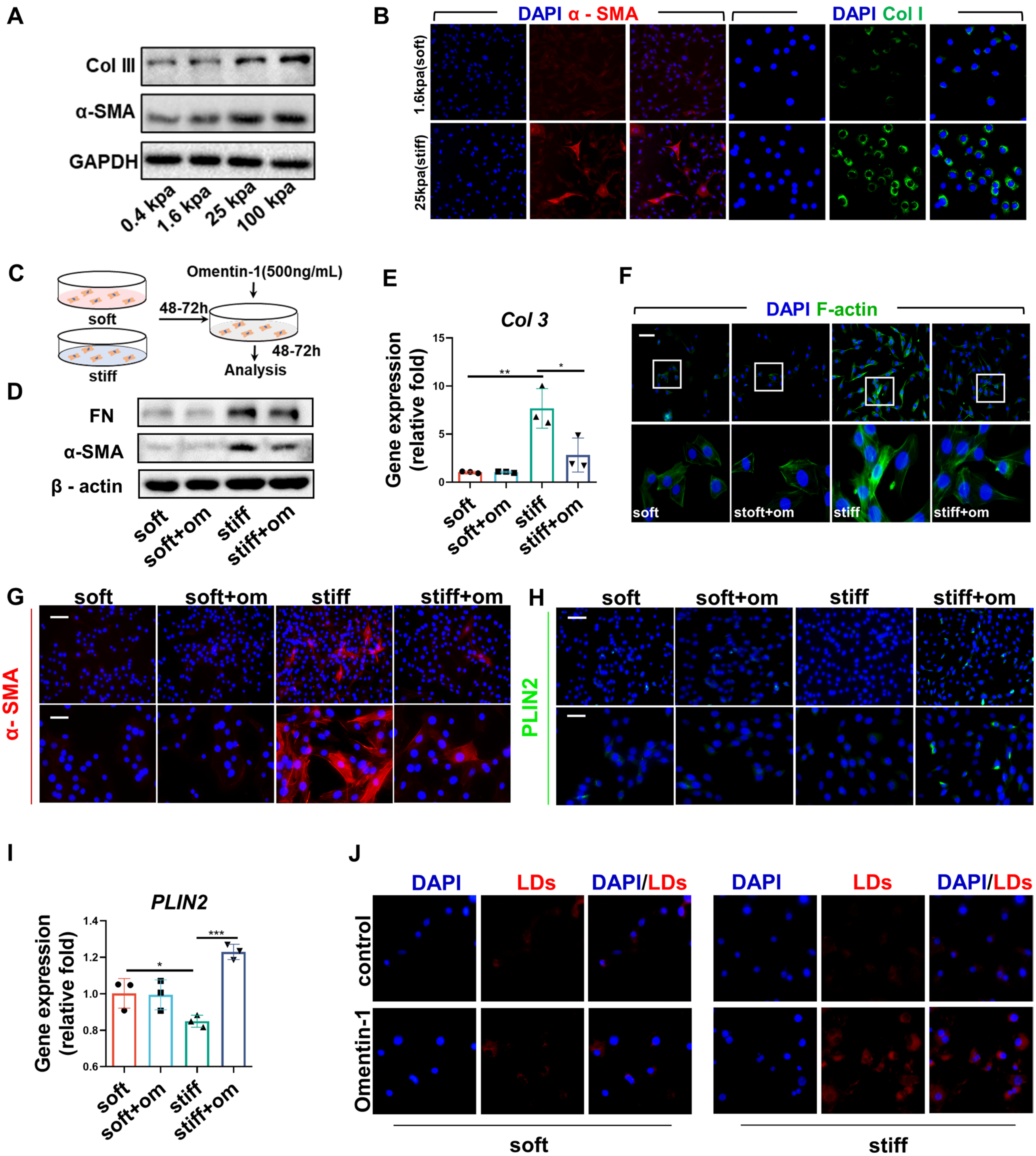

Fig. 4 Omentin-1 promotes myofibroblast lipogenic differentiation in vitro. (**a**) The content of Col 3 and α-SMA expression in fibroblasts cultured on 0.4, 1.6, 25 and 100 kpa hydrogels detected by western blotting, GAPDH was used as the loading control ($n=3$). (**b**) Immunofluorescent staining of α-SMA (Red) (scale bar = 50 μm) and Col1 (Green) (scale bar = 25 μm) in fibroblasts cultured on 1.6 kpa (soft) and 25 kpa (stiff) hydrogels ($n=3$). (**c**) Schematic for fibroblasts activated by stiff matrix and treated with omentin-1. (**d**) The content of FN and α-SMA in fibroblasts detected by western blotting, β-actin was used as the loading control ($n=3$). (**e**) The mRNA level of Col 3 in fibroblasts detected by qPCR ($n=3$). (**f**) Phalloidin staining of F-actin in fibroblasts, scale bar = 50 μm ($n=3$). (**g, h**) Immunofluorescent staining of α-SMA (Red) and PLIN2 (Green) in fibroblasts, up panel: scale bar = 50 μm, low panel: scale bar = 25 μm ($n=3$). (**i**) The mRNA level of PLIN2 in fibroblasts detected by qPCR ($n=3$). (**j**) Staining of Lipid droplets with Nile red in fibroblasts, scale bar = 25 μm ($n=3$)

characteristic of lipofibroblast (Fig. 4j). These results further certificate that omentin-1 promotes myofibroblasts deactivated into lipofibroblast cells.

Omentin-1 promotes myofibroblasts lipogenic differentiation by inhibiting PKM2-YAP signaling

In IPF, there is evidence of upregulation of glycolytic pathways [22, 23]. The glycolytic enzyme PKM2 has been found to regulate fibrosis development and progression by controlling glycine auxotrophy in myofibroblasts [24] and contributes to mechanical ventilation-induced pulmonary fibrosis [25]. In BLM pulmonary fibrosis mice, both mRNA and protein level of glycolytic enzymes, such as hexokinase 2 (HK2) and lactate dehydrogenase (LDHA), and in particular, PKM2, were increased in fibrotic lung tissue, in both reversible and non-reversible fibrosis models (Fig. 5a, b; Fig. S2A–D). In the fibrosis-resolved phase, the expression of these genes decreased and was further expedited by omentin-1 (Fig. 5a, b; Fig. S2A–D). PKM2 has either a tetramer configuration with high activity in controlling glucose oxidation or a dimer configuration with low activity in promoting glycolysis and biosynthesis, both of which can be transformed to the other [26, 27]. The active PKM2 tetramer form protects lung fibroblasts from fibrosis progression by decreasing collagen metabolism [24]. It should be noted that in the process of fibrosis, the tyrosine-activation of PKM2 in fibroblasts controls energy metabolism and cell differentiation. In particular, the phosphorylation of Y105 promotes the formation of dimeric PKM2 [28], leading to a glucose flux into aerobic glycolysis and activating fibroblast trans-differentiated into myofibroblasts [29]. Immunohistochemical analysis demonstrated increased PKM2 and phosphorylation of PKM2 Y105 in fibrotic lung tissue that was reversed by omentin-1 overexpression (Fig. 5c). These results lead us to hypothesize that omentin-1 instigates redistribution of PKM2 dimers and tetramers to reverse myofibroblasts activation or assists in the lipogenic differentiation pathway. To further interrogate whether the inhibition of glycolysis underlies the therapeutic effects of omentin-1 on lipogenesis in vitro (Fig. 5d), the protein levels of the glycolytic enzymes HK2, PKM2, and LDHA were analyzed. The upregulation of glycolytic enzymes in myofibroblasts induced by high stiffness was inhibited by omentin-1 (Fig. 5e). A significant increase in the PKM2 dimer proportion was demonstrated in myofibroblasts cultured on a stiff substrate, which was reversed by omentin-1 (Fig. 5f). The PKM2 dimer has been reported to be translocated into the nucleus, binding to the transcription factor YAP associated with matrix stiffness [29, 30]. The immunoblotting results indicated that omentin-1 substantially decreased the total YAP protein level in stiff matrix-activated myofibroblasts (Fig. 5g) and promoted the translocation of PKM2 and YAP from the cytoplasm to the nucleus (Fig. 5h). And the immunofluorescent staining showed that PKM2 was localized in the cytoplasm on a soft substrate, while on a stiff substrate there was a strong fluorescent signal overlapping with the nucleus (Fig. S2E). Furthermore, omentin-1 restricts the accumulation of nuclear YAP induced by high matrix stiffness (Fig. S2F). In addition, co-immunoprecipitation analyses showed that omentin-1 administration inhibited the stiffness-induced interaction between PKM2 and YAP (Fig. 5i). Colocalization of the PKM2 and YAP immunofluorescence signals in the myofibroblasts nucleus were intensified by high matrix stiffness, which was reversed by omentin-1 (Fig. 5j). These results demonstrate that in myofibroblasts activated by a stiff substrate, omentin-1 may prevent the interaction of the PKM2 dimer with YAP and restrict PKM2/YAP translocation activity to promote lipogenic differentiation of myofibroblasts.

To investigate whether inhibition of YAP underlies the lipogenic effects of omentin-1 in cells, we generated a YAP-overexpression plasmid (Fig. 5k). Overexpression was confirmed by the upregulation of YAP mRNA levels (Fig. S2G). YAP overexpression diminished the inhibitory effects of omentin-1 on myofibroblasts numbers and enhanced the effect of lipogenesis (Fig. 5l, m; Fig. S2G). These results demonstrate that overexpression of YAP reverses the effect of omentin-1 on the lipogenic differentiation of myofibroblasts. Additionally, the suppression of mRNA expression of aSMA was significantly observed upon the knockdown of YAP using small interfering RNA, while the gene expression of PLIN2 and intracellular lipid droplets increased (Fig. S2H–J). Interestingly, our metabolomic data revealed an upregulation of the glycolytic intermediates of FBP when cells were treated with omentin-1 on stiff substrates (Fig. 5n). It has been shown that FBP inhibits the phosphorylation of Y105 [28] and can trigger a reversible dimer-to-tetramer conversion of PKM2 to allosterically activate PKM2 [31]. FBP supplementation (Fig. 5o) significantly inhibited the combination of PKM2 and YAP (Fig. 5p) and reduced the mRNA level of Col 1 and YAP (Fig. 5q; Fig. S2K). Additionally, FBP upregulated gene expression of PLIN2 in stiffness-activated myofibroblasts (Fig. 5r). Together, the above results demonstrate that omentin-1 inhibits the PKM2 dimer by upregulating FBP to prevent the binding to YAP, ultimately promoting myofibroblasts lipogenic differentiation.

Omentin-1 leads myofibroblasts lipogenic differentiation by activating PPARγ signaling

PPARγ is a crucial regulator during lipogenic differentiation. Our results demonstrated that PPARγ was decreased in fibrotic lung tissue and reversed by omentin-1 overexpression both in reversible mole and non-reversible models (Fig. 6a, c–e; Fig. S6A, B) and there is a significant direct correlation

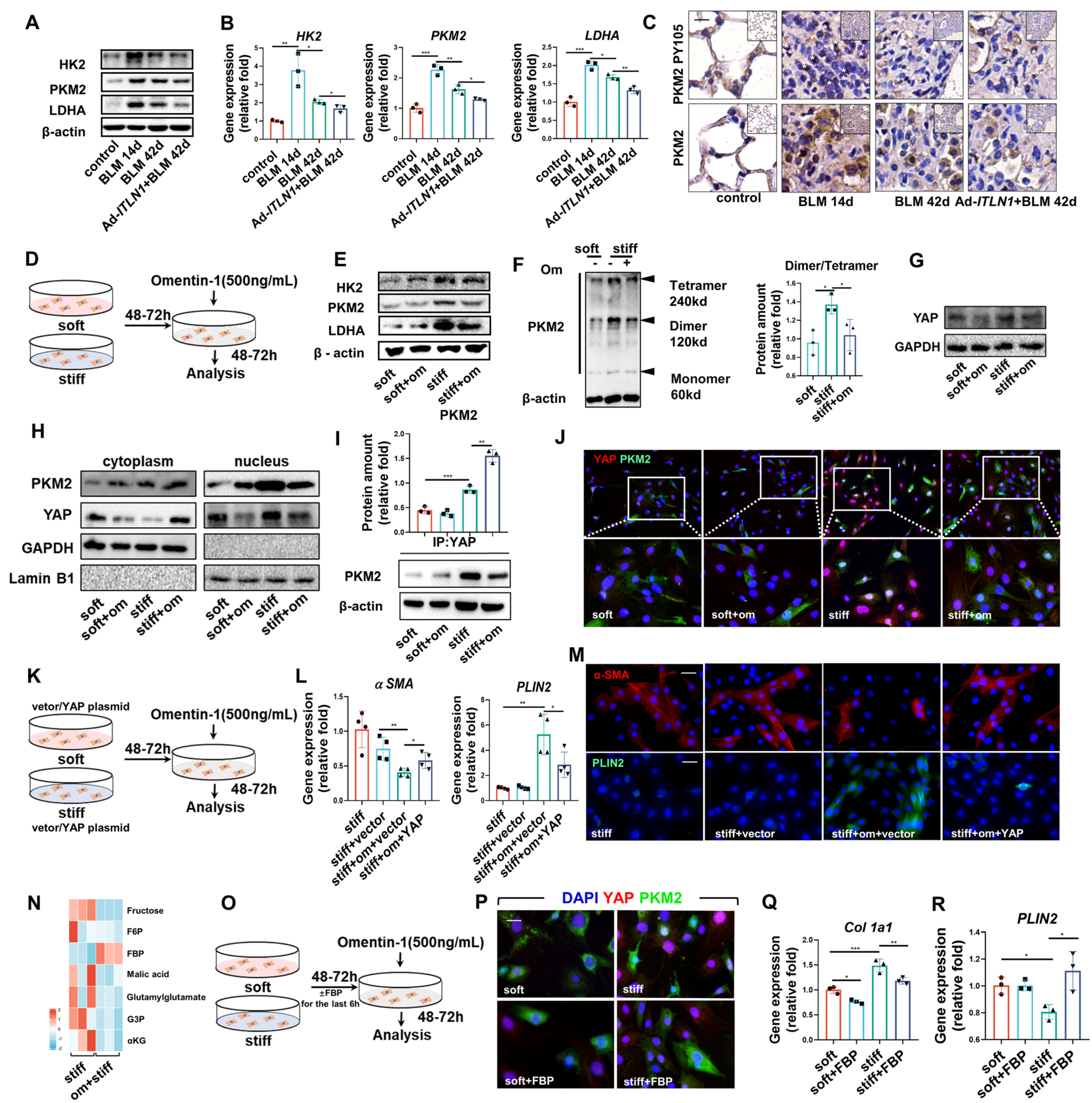

between omentin-1 and PPARγ (Fig. 6B; Fig. S6A, B). Concordantly, stiff substrate stimulation resulted in the downregulation of PPARγ, which was significantly reversed by omentin-1 administration (Fig. 6f). As we previously demonstrated the ability of omentin-1 promotes lipogenesis via inhibiting PKM2-YAP signaling, we conducted further investigation into the impact of YAP on the regulation of PPARγ through the overexpression or knockdown of YAP (Fig. 6g). Overexpression of YAP was observed to successfully counteract the influence of omentin-1 on increasing PPARγ gene expression and PPARγ Ser112 phosphorylation, which as demonstrated in previous research, regulates the lipogenic differentiation of pulmonary myofibroblasts [9]. Conversely, the knockdown of YAP led to increased PPARγ phosphorylation (Fig. 6h, i). Furthermore, inhibition of PPARγ with a specific inhibitor GW9662 (Fig. 6j) reversed the effect of omentin-1 in reducing the number of myofibroblasts, ECM deposition and in promoting lipofibroblasts differentiation (Fig. 6k–m). These results indicate that omentin-1 promotes myofibroblasts lipogenic differentiation by activating PPARγ through inhibition of the PKM2-YAP signaling pathway.

◂**Fig. 5** Omentin-1 restrains PKM2/YAP translocation activity and contributes to myofibroblast lipogenic differentiation. (**a**) The content of HK2, PKM2 and LDHA in the reversible fibrotic lung tissue of mice detected by western blotting, β-actin was used as the loading control ($n=3$). (**b**) The mRNA level of HK2, PKM2 and LDHA mRNA level in the reversible fibrotic lung tissue of mice detected by qPCR ($n=3$). (**c**) Immunohistochemistry staining of PKM2 and phosphorylation of PKM2 Y105 (Red asterisks) in the reversible fibrotic lung tissue of mice, scale bar = 25 μm ($n=3$). (**d**) Schematic for fibroblasts activated by stiff matrix and treated with omentin-1. (**e**) The content of HK2, PKM2 and LDHA expression in fibroblasts detected by western blotting, β-actin was used as the loading control ($n=3$). (**f**) The PKM2 dimer and tetramer formation in fibroblasts on soft, stiff matrix and treated with omentin-1. (**g**) The content of YAP expression in fibroblasts detected by western blotting, GAPDH was used as the loading control ($n=3$). (**h**) The content of PKM2 and YAP in the cytoplasm and nucleus of fibroblasts detected by western blotting, GAPDH or Lamin B1 was used as the loading control ($n=3$). (**i**) The interaction between endogenous YAP and PKM2 in fibroblasts detected by coimmunoprecipitation assay. (**j**) Intranuclear colocalization of endogenous YAP and PKM2 in fibroblasts detected by immunofluorescent staining, scale bar = 25 μm ($n=3$). (**k**) Schematic for fibroblasts activated by stiff matrix transfected with specific plasmid and treated with omentin-1. (**l**) The mRNA level of α-SMA and PLIN2 in the negative control (vector) or YAP plasmid transfected fibroblasts detected by qPCR ($n=4$). (**m**) Immunofluorescent staining of α-SMA and PLIN2 in transfected fibroblasts, scale bar = 50 μm ($n=3$). (**n**) Metabonomic analysis in fibroblasts on stiff matrix ($n=3$). (**o**) Schematic for fibroblasts activated by stiff matrix replenished with FBP and treated with omentin-1. (**p**) Intranuclear colocalization of endogenous YAP and PKM2 in fibroblasts treated with FBP detected by immunofluorescent staining. scale bar = 25 μm ($n=3$) (**q, r**) The mRNA level of Col 1 and PLIN2 mRNA level in fibroblasts following FBP treatment detected by qPCR ($n=3$)

Omentin-1 eventually reverses pulmonary fibrosis by regulating collagen synthesis and degradation

The balance between collagen synthesis and the degradation of myofibroblasts mediates the repair of lung injury, and the progression and regression of fibrosis [32–34]. Single-cell transcriptomics and recent studies show that lipofibroblasts are a phenotype that is poorly differentiated and less collagen-synthesizing [10–12]. Our results showed that the collagen synthesis gene lysyl oxidase-like 4 (LOXL4) mRNA was upregulated and the collagen degradation-related genes cathepsin K (CTSK), tissue-type plasminogen activator (PLAT) and matrix metallopeptidase 14 (MMP14) were downregulated in activated myofibroblasts while omentin-1 reverses these conversions (Fig. 7a). Metabolomics analysis also indicated that omentin-1 reduces the quantity of metabolites involved in the synthesis of collagen or promotion of fibrosis such as proline, threonine, hydroxylysine, etc., and increased the quantity of collagen degradation metabolites such as glycylproline and H-Gly-Pro-OH (Fig. 7b). Overexpression of YAP and pharmacological inhibition of PPARγ reversed the effects of omentin-1 on collagen synthesis and degradation-related genes respectively (Fig. 7c, d). In vivo, our results showed that lysyl oxidase-like 3 (LOXL3) and LOXL4 mRNA increased at the peak of fibrosis, but decreased during the resolving phases, and omentin-1 further reduces the mRNA levels of LOXL3 and LOXL4 (Fig. S3A), indicating that collagen synthesis gene expression decreases significantly during the fibrosis regression phases and omentin-1 further augments it. In contrast, collagen degradation gene expression increased at 42 d.p.i., and omentin-1 further increases their expression (Fig. S3B). Collagen hybridization peptide (CHP) is a synthetic peptide that can specifically bind to degraded and denatured collagen molecules, but not to intact collagen [35]. Omentin-1 reduces intact Col 1 in fibrotic lung tissue while the fluorescence intensity of CY3-CHP labeled denatured collagen strands were upregulated following omentin-1 administration (Fig. 7e), indicating that omentin-1 inhibits collagen deposition and promotes collagen degradation. In the non-reversible fibrosis model also showed that omentin-1 decreases collagen synthesis genes (Fig. S3C, D) and intact Col 1 (Fig. 7f, g), while increasing the collagen degradation genes (Fig. S3C, D) and denatured collagen strands (Fig. 7f, g) eventually inhibiting collagen deposition. The above data indicate that omentin-1 could decrease collagen synthesize and increase collagen degradation both in vivo and in vitro by inducing myofibroblasts lipogenic differentiation.

In addition, we reanalyzed the single-cell RNA sequencing (scRNA-seq) data of pulmonary fibrosis (Gene Expression Omnibus accession number GSE135893) and annotated clusters using lineage-defining markers to recover 31 cell types in the lung (Fig. 7g). Three subtypes including fibroblasts, myofibroblasts and PLIN2$^+$ fibroblasts were screened from the reconstructed human IPF mesenchymal cell populations (Fig. 7f). The expression of fibrotic genes (FN1, COL3A1, TGFβ1, ACTA2 and COL1A1) and collagen synthesis-related gene LOXL4 were significantly lower in PLIN2$^+$ fibroblasts compared with myofibroblasts in IPF lung. On the contrary, the expression of lipogenic differentiation genes (PPARγ, CEBPA and PLIN2) and collagen degradation-related genes (MMP12, PLAU, CTSK, PLAT) were significantly higher in PLIN2$^+$ fibroblasts compared with myofibroblasts (Fig. 7i). Together, these results demonstrated that lipofibroblasts were relatively quiescent deactivated cells with lower collagen synthesis ability and higher collagen degradation abilities.

Disscussion

In this study, we demonstrate that omentin-1 was significantly increased in lung tissue following BLM stimulation and the level of omentin-1 is negatively correlated with the degree of fibrosis, indicating that omentin-1 is an endogenous adipokine that may participate in the resolution of fibrosis. Exogenous overexpression of omentin-1, mediated

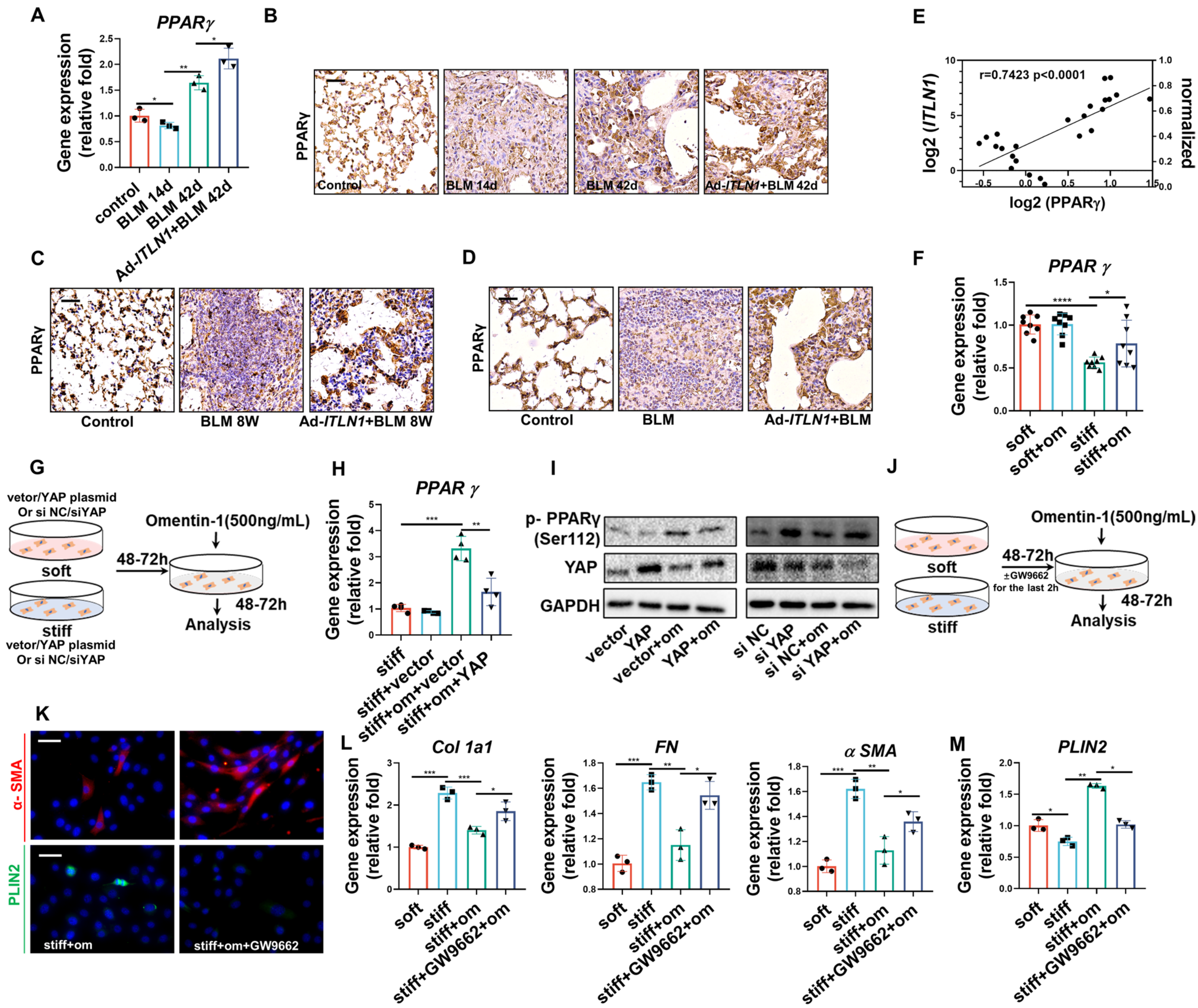

Fig. 6 PPARγ mediates myofibroblasts lipogenic pathway promoted by omentin-1. (**a**) The mRNA level of PPARγ in the reversible fibrotic lung tissue of mice detected by qPCR ($n=3$). (**b–d**) Immunohistochemistry staining of PPARγ in the reversible and non-reversible fibrotic lung tissue of mice, scale bar = 50 µm ($n=3$). (**e**) The correlation between PPARγ and omentin-1 mRNA levels in the reversible fibrosis model. (**f**) The mRNA level of PPARγ in fibroblasts detected by qPCR ($n=6$). (**g**) Schematic for fibroblasts activated by stiff matrix transfected with specific plasmid or siRNA and treated with omentin-1. (**h**) The mRNA level of PPARγ in negative control (vector) or YAP plasmid transfected fibroblasts detected by qPCR ($n=4$). (**i**) Western blot showing the inhibition or induction of PPARγ phosphorylation in response to YAP overexpression or knockdown treatment with/without omentin-1, GAPDH was used as the loading control ($n=3$). (J) Schematic for fibroblasts activated by stiff matrix and treated with GW9662 (a selective PPARγ inhibitor) and omentin-1 (**k**) Immunofluorescent staining of α-SMA and PLIN2 in fibroblasts following omentin-1 and GW9662 treatment, scale bar = 25 µm ($n=3$). (**l, m**) The mRNA level of Col 1, FN, α-SMA and PLIN2 in fibroblasts following omentin-1 and PPARγ inhibitor (GW9662) treatment detected by qPCR ($n=3$)

by adenovirus, significantly accelerated the regression of reversible pulmonary fibrosis and promoted the resolution of non-reversible pulmonary fibrosis. We demonstrate that omentin-1 strongly promotes myofibroblast trans-differentiation to the lipofibroblast, phenotype, with the associated reduction of collagen synthesis and the upregulation of collagen degradation in both reversible and non-reversible pulmonary fibrosis models. For detail mechanisms, we showed that omentin-1 significantly increases the level of metabolite FBP, which further reduces the PKM2 dimer, PKM2-YAP binding, and nuclear translocation in myofibroblasts. Decreased PKM2-YAP binding and nuclear translocation induced by omentin-1 upregulates and activates the lipogenic differentiation regulator PPARγ, promoting myofibroblasts deactivation into lipofibroblasts. Collectively,

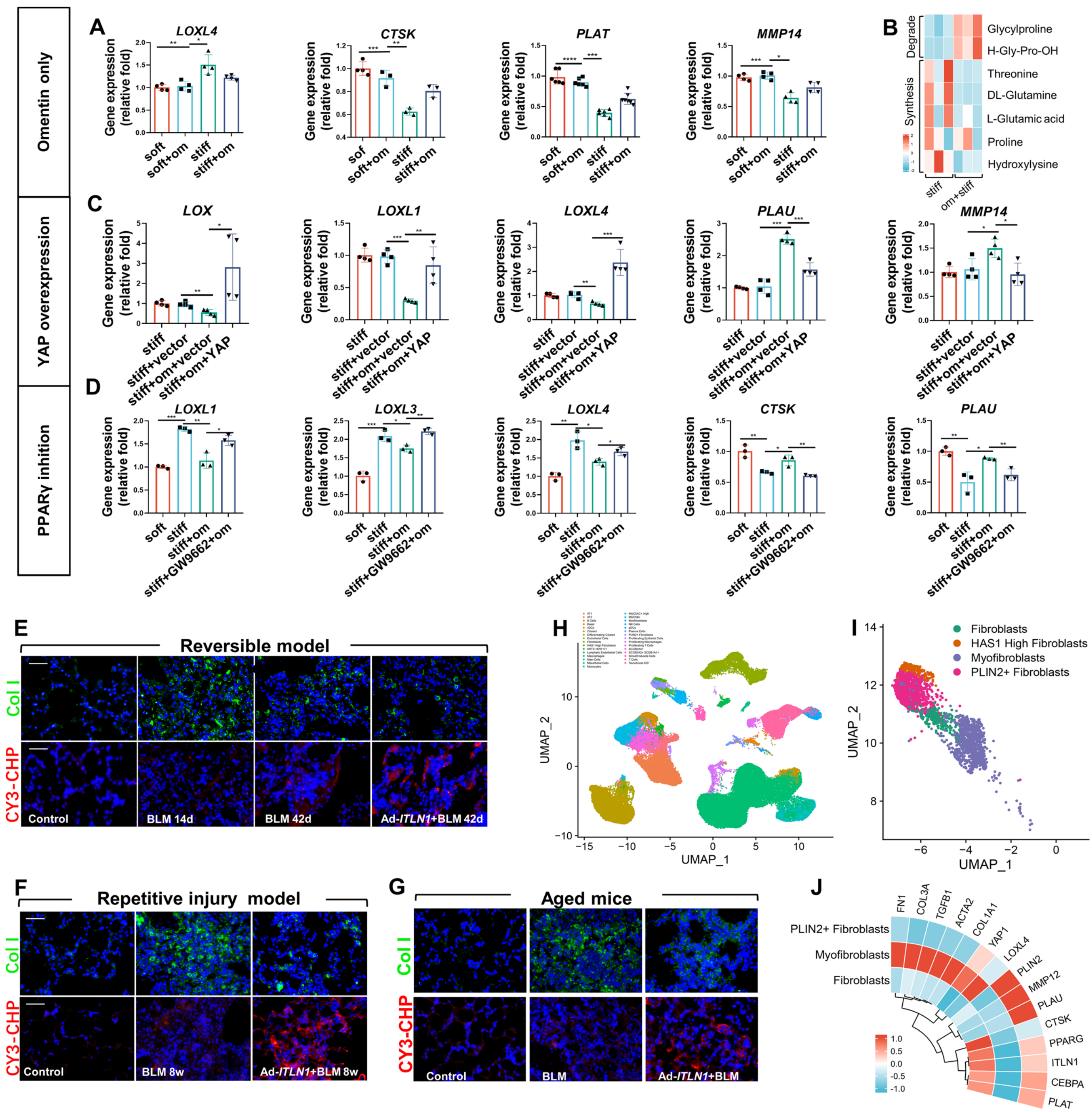

Fig. 7 Omentin-1 eventually reverses pulmonary fibrosis through decrease collagen synthesis and increased collagen degradation. (**a**) The mRNA level of ECM synthesis and degradation-associated genes in fibroblasts detected by qPCR ($n \geq 3$). (**b**) Metabonomic analysis of collagen degrading and synthetic metabolites in fibroblasts ($n=3$). (**c**) The mRNA level of ECM synthesis and degradation-associated genes in negative control (vector) or YAP plasmid transfected fibroblasts ($n=4$) detected by qPCR. (**d**) The mRNA level of ECM synthesis and degradation-associated genes in fibroblasts following omentin-1 and PPARγ inhibitor (GW9662) treatment detected by qPCR ($n=3$). (**e–g**) Immunofluorescent staining of intact collagens and degraded collagens in the reversible and nonreversible BLM injured fibrotic lung tissue, scale bar = 50 μm ($n=3$). (**h**) Cell type in human PF lungs. (**i**) UMAP depicting mesenchymal cells from jointly analyzed human PF lungs. (**j**) Normalized expression levels of differential genes in human PF fibroblasts, myofibroblasts, and PLIN2$^+$ fibroblasts

our results advocate the therapeutic potential of exogenous omentin-1 in treating established lung fibrosis (Fig. 8).

Omentin-1 is a novel hydrophilic adipokine of 313 amino acids (35 kDa) which has been found to exert important anti-inflammatory, antioxidative and anti-apoptotic roles and also demonstrates protective effects against cancer, atherosclerosis, type 2 diabetes mellitus, and bone metabolic diseases [13, 36]. BLM-induced pulmonary fibrosis in mice

Fig. 8 Schematic of a model of the antifibrotic mechanism of omentin-1 on pulmonary fibrosis

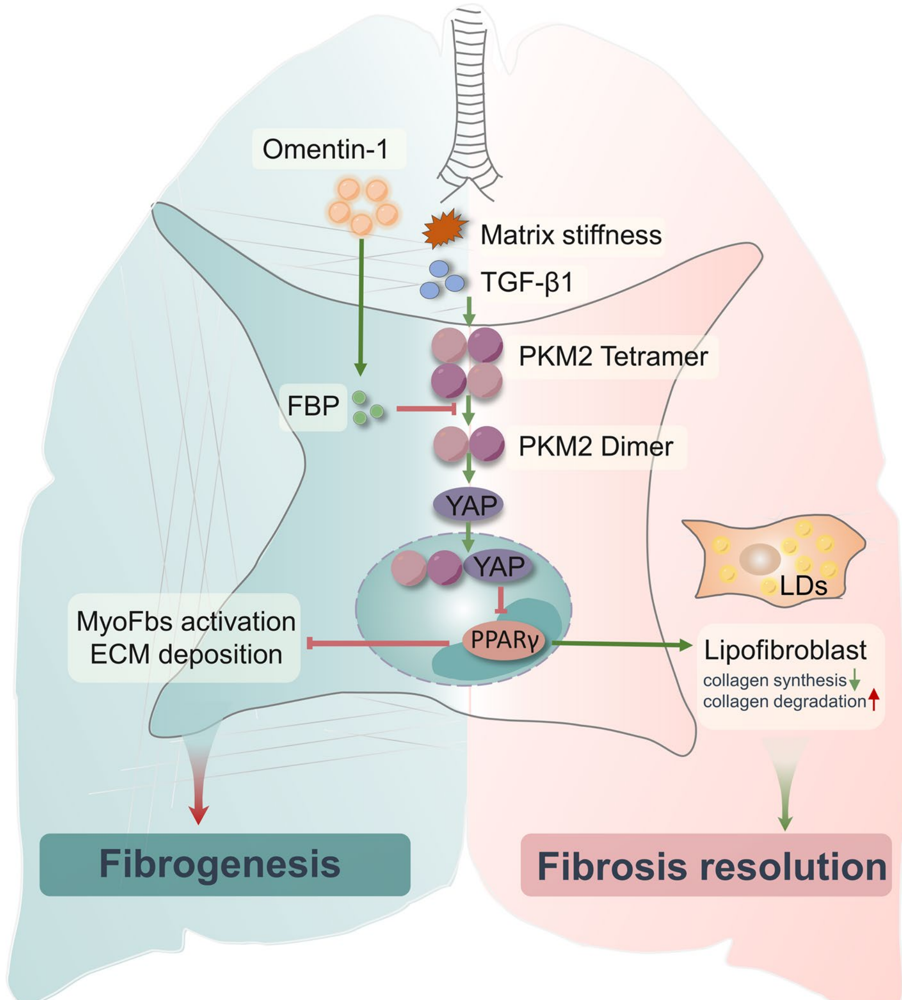

has been widely used in the study of pulmonary fibrosis [37, 38]. In the single-dose BLM model, there is a spontaneous resolution of the fibrosis beginning around day 14–21 following the BLM challenge [15]. Our previous study showed that omentin-1 levels increase at 14 and 21 d.p.i. However, omentin-1 deletion exacerbated BLM-induced pulmonary fibrosis, and overexpression of omentin-1 attenuated pulmonary fibrosis [17], which indicated us that omentin-1 could be a potential endogenous antifibrosis drug that functions by reducing the number of myofibroblasts via activation of the adenosine 3′,5′-monophosphate activated protein kinase pathway. In this study, we further demonstrate that omentin-1 was significantly increased in regressive fibrotic lungs at 42 d.p.i., when the degree of fibrosis has been largely resolved. Importantly, the level of omentin-1 is negatively correlated with the degree of fibrosis respectively at 14, 21, and 42 d.p.i. We demonstrated that overexpression of omentin-1 significantly accelerates the regression of reversible pulmonary fibrosis at 42 d.p.i. These results indicate that omentin-1 is an endogenous anti-fibrosis factor secreted following BLM injury, that can accelerate the resolution of reversible pulmonary fibrosis. However, human fibrotic lung diseases, such as IPF, likely develop following a series of repeated injuries culminating in progressive disease, which is irreversible. Therefore, a model using a single-dose of injury does not adequately reflect events that occurs in IPF [38]. Repetitive lung injury with BLM produces substantial architectural distortion in the lungs and fibrosis that does not spontaneously resolve [20]. In addition, pulmonary fibrosis generally manifests in individuals 55 years and older, suggesting that IPF is a disease associated with aging [39, 40]. Researches has shown that aged mice also develop a deficiency in their capacity for lung fibrosis resolution in response to BLM [15]. These two models are non-resolved models that more closely resemble IPF than the single intratracheal instillation of BLM-induced lung fibrosis model. Our study showed that overexpression of omentin-1 significantly attenuates pulmonary fibrosis in these two non-reversible models. Thus, the antifibrotic effects of omentin-1 were comprehensively demonstrated using different pulmonary fibrosis models.

Lipofibroblasts are characterized by a large volume of lipid bodies and localization in the alveolar interstitium, often at the base of the septa and in close proximity to alveolar epithelial type 2 cells. It is a resident fibroblast that contributes to the myofibroblast phenotype during pulmonary fibrosis [41]. In contrast, during fibrosis resolution, lineage-labeled activated myofibroblasts, labeled using the Tg (Acta2-CreERT2), do not undergo apoptotic clearance, but instead transdifferentiate back to the lipofibroblasts phenotype [12]. Furthermore, lipofibroblasts obtained from myofibroblasts ex vivo in precision cut lung slices from end-stage IPF lungs from transplant patients, mediate the potential role of metformin in reversing fibrosis [9]. Transdifferentiation of myofibroblasts into lipofibroblasts is an effective method to reverse pulmonary fibrosis [9, 12]. The results we present here build upon our previous studies on the therapeutic effects of omentin-1 on pulmonary fibrosis by reducing the number of SA100A4 and α-SMA double-positive cells in the BLM injured 28 d.p.i. fibrotic lungs [17]. In this study, we observed that the number of myofibroblasts decreased while the number of lipofibroblasts increased significantly during BLM injury 42 d.p.i., that is, during the fibrosis regression phase, which is consistent with the previous findings [12]. In addition, omentin-1 accelerates the decrease in myofibroblasts and the corresponding emergence of lipofibroblasts. Moreover, two non-reversible models were established, and it was found that omentin-1 could still increase the number of lipofibroblasts to alleviate pulmonary fibrosis in these models too. Single-cell transcriptomics and recent studies have shown that lipofibroblasts are a poorly differentiated phenotype that synthesize less collagen than myofibroblasts [10–12]. Our results showed that in both the reversible and non-reversible pulmonary fibrosis models, omentin-1 promotes the formation of lipofibroblasts, accompanied by decreased collagen synthesis and increased collagen degradation abilities.

IPF is characterized by progressive fibroblast proliferation and myofibroblast activation, along with extensive ECM deposition of ECM. Myofibroblasts play a crucial role in ECM deposition. TGF-β1 is involved in myofibroblast differentiation and is an accepted method for the creation of a profibrotic microenvironment and fibroblast activation. ECM is both a cause and a consequence of fibroblast activation because increased ECM stiffness is strongly associated with profibrotic changes in cell phenotype and differentiation. The accumulation of ECM by myofibroblasts constitutes a stiff profibrotic environment that promotes the continuous activation of fibroblasts [18, 32]. Polyacrylamide hydrogel mimics this positive feedback loop in vitro and provides a pre-activated myofibroblast state. Our previous results demonstrated that omentin-1 pretreatment reduces the expression of α-SMA and ECM components in TGF-β1 stimulated-activated myofibroblasts [17]. In this study, we observed that omentin-1 promotes lipogenic differentiation of activated myofibroblasts induced by TGF-β1 or high stiffness, indicated by a decreased level of α-SMA, and increased levels of the lipogenic differentiation marker PLIN2 and lipid droplets.

ECM production and degradation in normal lung tissues are in a homeostasis and fibrosis may develop if this balance is disrupted. The production and deposition of ECM components are an important characteristic of lung fibrosis [5]. Matrix and collagen degradation are necessary for fibrosis resolution, which is closely related to the spontaneous resolution of BLM-induced pulmonary fibrosis in animal models [37, 42]. Therefore, the reduction of collagen deposition includes changes in collagen synthesis and degradation enzymes. Importantly, the presence of degraded collagen or collagen degradation products is a decisive basis for the resolution of pulmonary fibrosis, characterizing their therapeutic effect on pulmonary fibrosis. Our results show that omentin-1 promotes myofibroblasts lipogenic differentiation, reduces the content of metabolites involved in collagen synthesis and increases the content of collagen degradation metabolites, further confirming that omentin-1 enables myofibroblasts to attain a dedifferentiated state. Furthermore, scRNA-seq reanalysis reavealed the existence of lipofibroblasts in human IPF lungs and that lipofibroblasts are relatively quiescent deactivated cells with lower collagen synthesis and enhanced collagen degradation abilities. These results verify that omentin-1 promotes lipogenic differentiation of myofibroblasts and regulates collagen turnover, thus promoting the resolution of pulmonary fibrosis.

In IPF, there is evidence of upregulation of glycolytic pathways [22]. Several rate-limiting enzymes involved in glycolysis, including fructose-2,6-biphosphatase 3 (PFKFB3), phosphofructokinase-1 (PFK-1), HK2 and PKM2, are significantly upregulated in activated lung fibroblasts [23, 24]. The glycolytic enzyme PKM2 has been proven to play an important role in the glycolysis pathway. It has either a tetramer configuration with high activity in controlling glucose oxidation or a dimer configuration with low activity in promoting glycolysis and biosynthesis, both of which can be transformed to the other [26, 27]. Phosphorylation at Y105 directly and transiently mediates FBP release from many PKM2 molecules to form dimer that are conducive to aerobic glycolysis [43, 44]. It has been shown that FBP inhibits phosphorylation of Y105, and an excess of FBP can convert the dimeric fraction of PKM2 to a tetramer [28, 31, 45]. The PKM2 dimer exhibits translocation activity, which affects the downstream signaling pathway after combining with the mechanosensitive transcriptional coactivators YAP. YAP responds to TGF-β1, mechanical signaling and glycolysis to regulate the activation of fibroblasts into myofibroblasts that highly expressed α-SMA to promote pulmonary fibrosis, suggesting activation of PKM2/YAP as a key underlying signaling event, leading to upregulation of α-SMA and collagen. We also demonstrated that omentin-1 increases the FBP metabolite, thus downregulating PKM2 pY105 and reducing the content ration of PKM2 dimers to tetramers. Our data illustrates that increased matrix stiffness enhances the interaction and colocalization of PKM2 and YAP in the nucleus, and omentin-1 suppresses this phenomenon. Overexpression of YAP reverses the effect of omentin-1 on lipogenic differentiation of myofibroblasts. Whereas knockdown of YAP promotes lipid droplet production in myofibroblasts. Moreover, FBP supplementation inhibits the collagen synthesis of myofibroblasts and upregulates the lipogenic differentiation marker PLIN2. These results show that increasing the level of FBP to inhibit PKM2 and YAP binding in the nucleus is a key point of the antifibrotic effect of omentin-1.

PPARγ is a lipofibroblast characteristic markers as well as a master switch of lipogenic differentiation in myofibroblasts [12]. Metformin significantly upregulates PPARγ and increases the phosphorylation of PPARγ protein at Ser112 and induces lipid-droplet accumulation in human IPF lung fibroblasts. PPARγ agonists have been shown to protect mice from developing BLM-induced lung fibrosis [46]. Furthermore, rosiglitazone, a PPARγ agonist antagonizes the TGF-β-mediated fibrotic phenotype [12]. Here, we show that PKM2-YAP signaling is inhibited in omentin-1-treated myofibroblasts, likely due to FBP upregulation. YAP senses mechanical stress in mesenchymal cells to regulate mesenchymal stem cells (MSCs) adipogenic or osteogenic and mediated MSCs transdifferentiating into adipocytes in soft matrix, YAP leads to MSCs displaying reduced expression of the adipocyte markers ADIPOQ, PPARγ, PLIN1 and failure to accumulate lipid droplets [47]. We also provide further insights into the mechanism by which omentin-1 promotes myofibroblasts lipogenic differentiation. Our results showed that reduction of PPARγ in fibrotic lungs and high matrix stiffness-activated myofibroblasts and omentin-1 restores it. Overexpression of YAP diminishes the effect of omentin-1 on promoting the expression and activation of the lipogenic differentiation regulator PPARγ, while knockdown of YAP promoted, PPARγ Ser112 phosphorylation, which was found to be involved in lipogenic differentiation of pulmonary myofibroblasts [9]. Further study by inhibition of PPARγ significantly reversed the effect of omentin-1 on lipogenic differentiation. Our data emphasize that omentin-1 induces lipogenic differentiation in myofibroblasts by PPARγ activation via inhibition of PKM2-YAP signaling.

In conclusion, this study demonstrates a clear antifibrotic role for omentin-1 in the lungs. Omentin-1 participates in the resolution of fibrosis by promoting myofibroblast transdifferentiation to lipofibroblasts, characterized by the reduction of collagen synthesis and the upregulation of collagen degradation in both reversible and non-reversible pulmonary fibrosis. Mechanistically, omentin-1 significantly increases the level of the metabolite FBP, which further reduces the PKM2 dimer and PKM2-YAP binding in myofibroblasts subsequently activating PPARγ, ultimately promoting myofibroblasts deactivation into lipofibroblasts. Our data highlight the potential that omentin-1 might be an alternative therapeutic option in treating IPF patients.

Supplementary Information The online version contains supplementary material available at https://doi.org/10.1007/s00018-023-04961-y.

Acknowledgements Not applicable.

Author contributions Conceptualization: ZYN, ZY, LZQ; Data curation: ZYN, ZY; Formal analysis: ZYN, ZY, LC; Investigation: ZYN, FJF, CYF, LXH, CHP; Project administration: LZQ, ZY, ZYN; Resources: LZQ, ZY, HY, FDD; Software: QYJ, SM; Supervision: LZQ, ZY, YSJ, ZWS; Validation: LZQ, ZY; Writing—original draft: ZYN, ZY and Writing—review & editing: ZYN, ZWS, ZY, LZQ.

Funding National Natural Science Foundation of China 82070068 (LZQ), National Natural Science Foundation of China 81870059 (LZQ), National Natural Science Foundation of China 82200085 (ZY), Natural Science Foundation of Changsha kq2202116 (ZY), and Central South University 2022ZZTS0837 (ZYN).

Data and materials availability RNA-seq and microarray data reanalyzed in the paper are in publicly available libraries from GEO under accession nos. GSE135893. All data associated with this study are present in the paper or the Supplementary Materials.

Declarations

Conflict of interest The authors declare that they have no known competing financial interests or personal relationships that could have appeared to influence the work reported in this paper.

Ethics approval and consent to participate The animal study protocol was approved by the ethics committee of the Central South University Science Research Center (Changsha, China) (protocol code: 2020sydw0715).

Consent for publication Not applicable.

References

1. Gross TJ, Hunninghake GW (2001) Idiopathic pulmonary fibrosis. N Engl J Med 345:517–525. https://doi.org/10.1056/NEJMra003200
2. Wakwaya Y, Brown KK (2019) Idiopathic pulmonary fibrosis: epidemiology, diagnosis and outcomes. Am J Med Sci 357:359–369. https://doi.org/10.1016/j.amjms.2019.02.013
3. King TE Jr, Bradford WZ, Castro-Bernardini S, Fagan EA, Glaspole I, Glassberg MK, Gorina E, Hopkins PM, Kardatzke D, Lancaster L et al (2014) A phase 3 trial of pirfenidone in patients with idiopathic pulmonary fibrosis. N Engl J Med 370:2083–2092. https://doi.org/10.1056/NEJMoa1402582
4. Distler O, Highland KB, Gahlemann M, Azuma A, Fischer A, Mayes MD, Raghu G, Sauter W, Girard M, Alves M et al (2019) Nintedanib for systemic sclerosis-associated interstitial lung

disease. N Engl J Med 380:2518–2528. https://doi.org/10.1056/NEJMoa1903076
5. Zhao X, Kwan JYY, Yip K, Liu PP, Liu FF (2020) Targeting metabolic dysregulation for fibrosis therapy. Nat Rev Drug Discov 19:57–75. https://doi.org/10.1038/s41573-019-0040-5
6. Zhang R, Jing W, Chen C, Zhang S, Abdalla M, Sun P, Wang G, You W, Yang Z, Zhang J et al (2022) Inhaled mRNA nanoformulation with biogenic ribosomal protein reverses established pulmonary fibrosis in a bleomycin-induced murine model. Adv Mater 34:e2107506. https://doi.org/10.1002/adma.202107506
7. Hinz B, Phan SH, Thannickal VJ, Galli A, Bochaton-Piallat ML, Gabbiani G (2007) The myofibroblast: one function, multiple origins. Am J Pathol 170:1807–1816. https://doi.org/10.2353/ajpath.2007.070112
8. Merkt W, Zhou Y, Han H, Lagares D (2021) Myofibroblast fate plasticity in tissue repair and fibrosis: deactivation, apoptosis, senescence and reprogramming. Wound Repair Regen 29:678–691. https://doi.org/10.1111/wrr.12952
9. Kheirollahi V, Wasnick RM, Biasin V, Vazquez-Armendariz AI, Chu X, Moiseenko A, Weiss A, Wilhelm J, Zhang JS, Kwapiszewska G et al (2019) Metformin induces lipogenic differentiation in myofibroblasts to reverse lung fibrosis. Nat Commun 10:2987. https://doi.org/10.1038/s41467-019-10839-0
10. Angelidis I, Simon LM, Fernandez IE, Strunz M, Mayr CH, Greiffo FR, Tsitsiridis G, Ansari M, Graf E, Strom TM et al (2019) An atlas of the aging lung mapped by single cell transcriptomics and deep tissue proteomics. Nat Commun 10:963. https://doi.org/10.1038/s41467-019-08831-9
11. Xie T, Wang Y, Deng N, Huang G, Taghavifar F, Geng Y, Liu N, Kulur V, Yao C, Chen P et al (2018) Single-cell deconvolution of fibroblast heterogeneity in mouse pulmonary fibrosis. Cell Rep 22:3625–3640. https://doi.org/10.1016/j.celrep.2018.03.010
12. El Agha E, Moiseenko A, Kheirollahi V, De Langhe S, Crnkovic S, Kwapiszewska G, Szibor M, Kosanovic D, Schwind F, Schermuly RT et al (2017) Two-way conversion between lipogenic and myogenic fibroblastic phenotypes marks the progression and resolution of lung fibrosis. Cell Stem Cell 20:261-273.e263. https://doi.org/10.1016/j.stem.2016.10.004
13. Zhou Y, Zhang B, Hao C, Huang X, Li X, Huang Y, Luo Z (2017) Omentin-A novel adipokine in respiratory diseases. Int J Mol Sci. https://doi.org/10.3390/ijms19010073
14. Raghow R, Lurie S, Seyer JM, Kang AH (1985) Profiles of steady state levels of messenger RNAs coding for type I procollagen, elastin, and fibronectin in hamster lungs undergoing bleomycin-induced interstitial pulmonary fibrosis. J Clin Invest 76:1733–1739. https://doi.org/10.1172/JCI112163
15. Hecker L, Logsdon NJ, Kurundkar D, Kurundkar A, Bernard K, Hock T, Meldrum E, Sanders YY, Thannickal VJ (2014) Reversal of persistent fibrosis in aging by targeting Nox4-Nrf2 redox imbalance. Sci Transl Med 6:231ra247. https://doi.org/10.1126/scitranslmed.3008182
16. Zhou Y, Hao C, Li C, Huang X, Li X, Tang Y, Huang Y, Tang S, Liu W, Feng D et al (2018) Omentin-1 protects against bleomycin-induced acute lung injury. Mol Immunol 103:96–105. https://doi.org/10.1016/j.molimm.2018.09.007
17. Zhou Y, Zhang Y, Cheng H, Li X, Feng D, Yue S, Xu J, Xie H, Luo Z (2022) Therapeutic effects of omentin-1 on pulmonary fibrosis by attenuating fibroblast activation via AMP-activated protein kinase pathway. Biomedicines. https://doi.org/10.3390/biomedicines10112715
18. Liu F, Lagares D, Choi KM, Stopfer L, Marinkovic A, Vrbanac V, Probst CK, Hiemer SE, Sisson TH, Horowitz JC et al (2015) Mechanosignaling through YAP and TAZ drives fibroblast activation and fibrosis. Am J Physiol Lung Cell Mol Physiol 308:L344-357. https://doi.org/10.1152/ajplung.00300.2014
19. Habermann AC, Gutierrez AJ, Bui LT, Yahn SL, Winters NI, Calvi CL, Peter L, Chung MI, Taylor CJ, Jetter C, et al (2020) Single-cell RNA sequencing reveals profibrotic roles of distinct epithelial and mesenchymal lineages in pulmonary fibrosis. Sci Adv 6:eaba1972. https://doi.org/10.1126/sciadv.aba1972
20. Degryse AL, Tanjore H, Xu XC, Polosukhin VV, Jones BR, McMahon FB, Gleaves LA, Blackwell TS, Lawson WE (2010) Repetitive intratracheal bleomycin models several features of idiopathic pulmonary fibrosis. Am J Physiol Lung Cell Mol Physiol 299:L442–L452. https://doi.org/10.1152/ajplung.00026.2010
21. Liu F, Mih JD, Shea BS, Kho AT, Sharif AS, Tager AM, Tschumperlin DJ (2010) Feedback amplification of fibrosis through matrix stiffening and COX-2 suppression. J Cell Biol 190:693–706. https://doi.org/10.1083/jcb.201004082
22. Kottmann RM, Kulkarni AA, Smolnycki KA, Lyda E, Dahanayake T, Salibi R, Honnons S, Jones C, Isern NG, Hu JZ et al (2012) Lactic acid is elevated in idiopathic pulmonary fibrosis and induces myofibroblast differentiation via pH-dependent activation of transforming growth factor-beta. Am J Respir Crit Care Med 186:740–751. https://doi.org/10.1164/rccm.201201-0084OC
23. Xie N, Tan Z, Banerjee S, Cui H, Ge J, Liu RM, Bernard K, Thannickal VJ, Liu G (2015) Glycolytic reprogramming in myofibroblast differentiation and lung fibrosis. Am J Respir Crit Care Med 192:1462–1474. https://doi.org/10.1164/rccm.201504-0780OC
24. Satyanarayana G, Turaga RC, Sharma M, Wang S, Mishra F, Peng G, Deng X, Yang J, Liu ZR (2021) Pyruvate kinase M2 regulates fibrosis development and progression by controlling glycine auxotrophy in myofibroblasts. Theranostics 11:9331–9341. https://doi.org/10.7150/thno.60385
25. Mei S, Xu Q, Hu Y, Tang R, Feng J, Zhou Y, Xing S, Gao Y, He Z (2022) Integrin beta3-PKM2 pathway-mediated aerobic glycolysis contributes to mechanical ventilation-induced pulmonary fibrosis. Theranostics 12:6057–6068. https://doi.org/10.7150/thno.72328
26. Nayak MK, Ghatge M, Flora GD, Dhanesha N, Jain M, Markan KR, Potthoff MJ, Lentz SR, Chauhan AK (2021) The metabolic enzyme pyruvate kinase M2 regulates platelet function and arterial thrombosis. Blood 137:1658–1668. https://doi.org/10.1182/blood.2020007140
27. Palsson-McDermott EM, Curtis AM, Goel G, Lauterbach MA, Sheedy FJ, Gleeson LE, van den Bosch MW, Quinn SR, Domingo-Fernandez R, Johnston DG et al (2015) Pyruvate kinase M2 regulates Hif-1alpha activity and IL-1beta induction and is a critical determinant of the warburg effect in LPS-activated macrophages. Cell Metab 21:65–80. https://doi.org/10.1016/j.cmet.2014.12.005
28. Wang P, Sun C, Zhu T, Xu Y (2015) Structural insight into mechanisms for dynamic regulation of PKM2. Protein Cell 6:275–287. https://doi.org/10.1007/s13238-015-0132-x
29. Srivastava SP, Li J, Kitada M, Fujita H, Yamada Y, Goodwin JE, Kanasaki K, Koya D (2018) SIRT3 deficiency leads to induction of abnormal glycolysis in diabetic kidney with fibrosis. Cell Death Dis 9:997. https://doi.org/10.1038/s41419-018-1057-0
30. Yamaguchi H, Taouk GM (2020) A potential role of YAP/TAZ in the interplay between metastasis and metabolic alterations. Front Oncol 10:928. https://doi.org/10.3389/fonc.2020.00928
31. Vander Heiden MG, Locasale JW, Swanson KD, Sharfi H, Heffron GJ, Amador-Noguez D, Christofk HR, Wagner G, Rabinowitz JD, Asara JM, Cantley LC (2010) Evidence for an alternative glycolytic pathway in rapidly proliferating cells. Science 329:1492–1499. https://doi.org/10.1126/science.1188015
32. Upagupta C, Shimbori C, Alsilmi R, Kolb M (2018) Matrix abnormalities in pulmonary fibrosis. Eur Respir Rev. https://doi.org/10.1183/16000617.0033-2018
33. McKleroy W, Lee TH, Atabai K (2013) Always cleave up your mess: targeting collagen degradation to treat tissue fibrosis. Am J

Physiol Lung Cell Mol Physiol 304:L709-721. https://doi.org/10.1152/ajplung.00418.2012
34. Glasser SW, Hagood JS, Wong S, Taype CA, Madala SK, Hardie WD (2016) Mechanisms of lung fibrosis resolution. Am J Pathol 186:1066–1077. https://doi.org/10.1016/j.ajpath.2016.01.018
35. Song S, Fu Z, Guan R, Zhao J, Yang P, Li Y, Yin H, Lai Y, Gong G, Zhao S et al (2022) Intracellular hydroxyproline imprinting following resolution of bleomycin-induced pulmonary fibrosis. Eur Respir J. https://doi.org/10.1183/13993003.00864-2021
36. Zhao A, Xiao H, Zhu Y, Liu S, Zhang S, Yang Z, Du L, Li X, Niu X, Wang C et al (2022) Omentin-1: a newly discovered warrior against metabolic related diseases. Expert Opin Ther Targets 26:275–289. https://doi.org/10.1080/14728222.2022.2037556
37. Yu QY, Tang XX (2022) Irreversibility of pulmonary fibrosis. Aging Dis 13:73–86. https://doi.org/10.14336/AD.2021.0730
38. Redente EF, Black BP, Backos DS, Bahadur AN, Humphries SM, Lynch DA, Tuder RM, Zemans RL, Riches DWH (2021) Persistent, progressive pulmonary fibrosis and epithelial remodeling in mice. Am J Respir Cell Mol Biol 64:669–676. https://doi.org/10.1165/rcmb.2020-0542MA
39. Selman M, Pardo A (2014) Revealing the pathogenic and aging-related mechanisms of the enigmatic idiopathic pulmonary fibrosis. an integral model. Am J Respir Crit Care Med 189:1161–1172. https://doi.org/10.1164/rccm.201312-2221PP
40. Mora AL, Rojas M, Pardo A, Selman M (2017) Emerging therapies for idiopathic pulmonary fibrosis, a progressive age-related disease. Nat Rev Drug Discov 16:755–772. https://doi.org/10.1038/nrd.2017.170
41. Schipke J, Kuhlmann S, Hegermann J, Fassbender S, Kuhnel M, Jonigk D, Muhlfeld C (2021) Lipofibroblasts in structurally normal, fibrotic, and emphysematous human lungs. Am J Respir Crit Care Med 204:227–230. https://doi.org/10.1164/rccm.202101-0043LE
42. Atabai K, Yang CD, Podolsky MJ (2020) You say you want a resolution (of fibrosis). Am J Respir Cell Mol Biol 63:424–435. https://doi.org/10.1165/rcmb.2020-0182TR
43. Hitosugi T, Kang S, Vander Heiden MG, Chung TW, Elf S, Lythgoe K, Dong S, Lonial S, Wang X, Chen GZ, et al (2009) Tyrosine phosphorylation inhibits PKM2 to promote the Warburg effect and tumor growth. Sci Signal 2:ra73. https://doi.org/10.1126/scisignal.2000431
44. Christofk HR, Vander Heiden MG, Wu N, Asara JM, Cantley LC (2008) Pyruvate kinase M2 is a phosphotyrosine-binding protein. Nature 452:181–186. https://doi.org/10.1038/nature06667
45. Nandi S, Razzaghi M, Srivastava D, Dey M (2020) Structural basis for allosteric regulation of pyruvate kinase M2 by phosphorylation and acetylation. J Biol Chem 295:17425–17440. https://doi.org/10.1074/jbc.RA120.015800
46. Genovese T, Cuzzocrea S, Di Paola R, Mazzon E, Mastruzzo C, Catalano P, Sortino M, Crimi N, Caputi AP, Thiemermann C, Vancheri C (2005) Effect of rosiglitazone and 15-deoxy-Delta 12,14-prostaglandin J2 on bleomycin-induced lung injury. Eur Respir J 25:225–234. https://doi.org/10.1183/09031936.05.00049704
47. Oliver-De La Cruz J, Nardone G, Vrbsky J, Pompeiano A, Perestrelo AR, Capradossi F, Melajova K, Filipensky P, Forte G (2019) Substrate mechanics controls adipogenesis through YAP phosphorylation by dictating cell spreading. Biomaterials 205:64–80. https://doi.org/10.1016/j.biomaterials.2019.03.009